Planta (2024) 260:38
https://doi.org/10.1007/s00425-024-04470-7

ORIGINAL ARTICLE

CaLAP1 and CaLAP2 orchestrate anthocyanin biosynthesis in the seed coat of *Cicer arietinum*

Samar Singh[1] · Lalita Pal[1] · Ruchika Rajput[1] · Himani Chhatwal[1] · Nidhi Singh[1] · Debasis Chattopadhyay[1] · Ashutosh Pandey[1]

Received: 22 December 2023 / Accepted: 17 June 2024 / Published online: 1 July 2024

Abstract

Main conclusion **Our findings shed light on the regulation of anthocyanin and proanthocyanidin biosynthesis in chickpea seed coats. Expression of R2R3-MYB transcription factors CaLAP1 and CaLAP2 enhanced the anthocyanins and proanthocyanidins content in chickpea.**

Abstract The seed coat color is a major economic trait in leguminous crop chickpea (*Cicer arietinum*). Anthocyanins and proanthocyanidins (PAs) are two classes of flavonoids that mainly contribute to the flower, seed coat and color of Desi chickpea cultivars. Throughout the land plant lineage, the accumulation of anthocyanins and PAs is regulated by MYB and bHLH transcription factors (TFs), which form an MBW (MYB, bHLH, and WD40) complex. Here, we report two R2R3-MYB TFs in chickpea belonging to the anthocyanin-specific subgroup-6, CaLAP1 (Legume Anthocyanin Production 1), and CaLAP2 (Legume Anthocyanin Production 2), which are mainly expressed in the flowers and developmental stages of the seeds. CaLAP1 and CaLAP2 interact with TT8-like CabHLH1 and WD40, forming the MBW complex, and bind to the promoter sequences of anthocyanin- and PA biosynthetic genes *CaCHS6, CaDFR2, CaANS,* and *CaANR,* leading to anthocyanins and PA accumulation in the seed coat of chickpea. Moreover, these CaLAPs partially complement the anthocyanin-deficient phenotype in the *Arabidopsis thaliana* sextuple mutant seedlings. Overexpression of *CaLAP*s in chickpea resulted in significantly higher expression of anthocyanin and PA biosynthetic genes leading to a darker seed coat color with higher accumulation of anthocyanin and PA. Our findings show that CaLAPs positively modulate anthocyanin and PA content in seed coats, which might influence plant development and resistance to various biotic and abiotic stresses.

Keywords Anthocyanin · Chickpea · Flavonoids · Legumes · MBW complex · MYB · Secondary metabolites

Abbreviations

ANR	Anthocyanidin reductase
ANS	Anthocyanidin synthase
CHS	Chalcone synthase
DFR	Dihydroflavonol 4-reductase
LAP	Legume anthocyanin production
LAR	Leucoanthocyanidin reductase
MBW	MYB–bHLH–WD40
PA	Proanthocyanidin
PAP	Production of anthocyanin pigment
TF	Transcription factor

Communicated by Dorothea Bartels.

Debasis Chattopadhyay
debasis@nipgr.ac.in

Ashutosh Pandey
ashutosh@nipgr.ac.in

[1] National Institute of Plant Genome Research, Aruna Asaf Ali Marg, New Delhi 110067, India

Introduction

Anthocyanins are water-soluble flavonoids with antioxidant properties responsible for coloration of flowers, seeds, and fruit in plants (Davies et al. 2012; Muñoz-Gómez et al. 2021; Jideani et al. 2021). Plant vegetative parts and trichomes accumulate anthocyanins, providing tolerance against biotic stresses such as pathogen attack and insect herbivory, as well as abiotic stresses like high light intensity and temperature fluctuations (Misra et al. 2010; Redondo-Gómez et al. 2013; Chen et al. 2019; Saxena et al. 2023a, b). Proanthocyanidins (PAs) are polyphenolic compounds abundant in plants. They are found in seeds, fruits, bark, leaves, and stems, contributing to the color, taste, and astringency of various plant-based foods and drinks (Samanta et al. 2011; Dasiman et al. 2022; Qi et al. 2023). PAs are integral to plant defense mechanisms against stresses such as pathogens and UV radiation (Hectors et al. 2012). They also play a role in seed coat formation and provide potential health benefits to both humans and animals (Bogs et al. 2005; Lattanzio et al. 2009; Mellway et al. 2009; Huang et al. 2010; Dixon et al. 2020). The flavonoid biosynthesis pathway consists of biosynthetic genes: *chalcone synthase* (*CHS), chalcone isomerase (CHI), flavanone-3-hydroxylase (F3H)*, *flavonoid 3'-hydroxylase (F3'H)*, *dihydroflavonol 4-reductase (DFR), anthocyanidin synthase (ANS), anthocyanidin reductase (ANR),* and *leucoanthocyanidin reductase (LAR)* that synthesize anthocyanins and PAs from dihydro flavonols (Pandey et al. 2016; Naik et al. 2024). Anthocyanins are temporally and spatially accumulated in different parts of the plants, and their biosynthesis is regulated by the heterotrimeric transcription factors MBW complex, composed primarily of R2R3-MYB, bHLH, and WD40 proteins (Carey et al. 2004; Li et al. 2016; Naik et al. 2021). MYB regulatory proteins consist of a DNA-binding domain at the N-terminal, while the C-terminal is responsible for interaction with other proteins (Ambawat et al. 2013). The MYB domain consists of three α-helices, each 50–60 amino acid-long imperfect repeats categorized as R1, R2, and R3 MYBs (Rajput et al. 2022b).

These R2R3-MYB TFs are plant-specific regulatory proteins that regulate various processes such as specialized metabolism, abiotic stress responses, defense, phytohormone signaling, root genesis, growth, and development in plants (Dixon and Paiva 1995; Dubos et al. 2010; Naik et al. 2022). The MBW complex is crucial for regulating anthocyanin biosynthesis across various plant species (Ramsay and Glover et al. 2005). Expression of these proteins from different species in *Arabidopsis* mutants with reduced anthocyanin content has successfully restored anthocyanin levels. In *A. thaliana*, regulation of the flavonoid biosynthesis pathway is well understood. AtMYB75 (PAP1), AtMYB90 (PAP2), AtMYB113 (PAP3), and AtMYB114 (PAP4) regulate anthocyanin biosynthesis in the model plant *Arabidopsis thaliana* (Borevitz et al. 2000; Zimmermann et al. 2004; Zuluaga et al. 2008; Bac-Molenaar et al. 2015). Despite extensive research on flavonoids in crops such as *Medicago*, apple, peach, and tomato over the years, the regulatory mechanisms in chickpea has still not been fully elucidated (Li et al. 2012; Pang et al. 2007; Tohge et al. 2017; Rajput et al. 2022b; Saxena et al. 2023a, b). Peel et al. (2009) identified and characterized an R2R3-MYB (MtLAP1) that regulates anthocyanin in *Medicago truncatula*. In another study, the interaction of MtTT8 with MtWD40-1, and MtPAR or MtLAP1 results in MBW complexes, which in turn activates *MtANS* and *MtANR* promoters for triggering anthocyanin and PA accumulation, respectively (Li et al. 2016). In *Cammelia sinensis,* the overexpression of *CsWD40* in *A. thaliana transparent testa glabra 1 (ttg1)* restored the normal trichome and seed coat developmental patterns (Liu et al. 2018). Co-expression of *CsWD40* and *CsMYB5e* in tobacco plants led to the accumulation of anthocyanins and PAs content. VvMYBA1 and VvMYBA2 are key regulators of anthocyanin biosynthesis in grape berries (Rinaldo et al. 2015). Also, the orthologs of these proteins, MdMYBA/MdMYB1/MdMYB10 and PcMYB10, regulate anthocyanin biosynthesis in apple and pear (*Pyrus communis*), respectively. MdMYB10 regulates anthocyanin accumulation in the fruit flesh and affects the skin color across many apple genotypes (Li et al. 2012; Hu et al. 2016). Although MdMYBA and MdMYB1 are expressed in the red-colored fruit skin in a few genotypes, a recent study unveils that MdMYB110a, a paralog of MdMYB10, also regulates anthocyanin accumulation in the flesh of apple (Fang et al. 2023). In the *Dendrobium* hybrid, DhbHLH and DhMYB interact to regulate spatial and temporal anthocyanin accumulation in floral tissues (Wang et al. 2022). This interaction ensures that anthocyanin pigments are precisely localized and expressed at specific developmental stages, contributing to the vibrant coloration of the flowers. In addition to the role of MYB TFs activating the anthocyanin and PA biosynthesis, they can also act as a repressor in many cases, such as MaMYBPR in banana, FaMYB1 in strawberries, and VvMYB4 in grapevines (Paolocci et al. 2011; Pérez-Daz et al. 2016; Rajput et al. 2022a, b). The MBW module consisting of FaMYB5, FaEGL3, and FaLWD1-like directly targets the promoters of *F3'H* and *LAR*, thereby regulating the content of anthocyanins and PAs (Yue et al. 2023). Through this coordinated action, the MBW complex ensures the precise modulation of these secondary metabolites for optimal plant health and productivity. APETALA2 (AP2) transcription factors (TFs) disrupt the formation of the MBW complex, resulting in the repression of PA biosynthesis.

Chickpea (*Cicer arietinum* L.) is an annual legume crop and the second-most cultivated pulse crop in terms of production and consumption (Koul et al. 2022). Cultivated chickpeas are of two types according to seed and flower morphology: Kabuli and Desi. The seed coat color is an important agronomic trait due to enriched flavonoid and other antioxidant dietary components in chickpea (Pal et al. 2023). The physical appearance of Kabuli seeds, such as light color and large size, has long been a trait of consumer preference and trade value, in addition to being an important quality target component and adaptation trait (Bajaj et al. 2015). Desi seeds are darker in color due to anthocyanin and PAs accumulation in the seed coat (Rajput et al. 2022b; Pal et al. 2023).

This study characterizes two anthocyanin-specific SG6 MYB TFs, CaLAP1, and CaLAP2 in chickpea. They interact with the TT8-like CabHLH1, forming a trimeric complex with CaTTG1 (WD40), potentially activating anthocyanin and PA biosynthesis genes. Further, *CaLAP1* and *CaLAP2* partially restored anthocyanin deficiency in Arabidopsis mutants and when overexpressed in chickpea, increased the accumulation of anthocyanin and PA in chickpea seed coats. These findings provide insight into anthocyanin and PA regulation in chickpea, offering the potential for developing varieties with higher anthocyanin and PA levels and improved stress tolerance.

Materials and methods

Plant material

Chickpea (*Cicer arietinum* L.) cultivars ICC4958 (*Desi type*) and ICCV2 (*Kabuli type*) plants were grown in the fields of the National Institute of Plant Genome Research (NIPGR), New Delhi, India. For genetic transformation, ICC4958 cultivar was used and grown in the plant growth chamber (Conviron, Winnipeg, Canada) at 22–24 °C with 60% humidity and a 10-h light period with an intensity of 250 µmol m^{-2} s^{-1}. Crossing a triple *myb* mutant *myb12, myb111, and myb11* (Stracke et al. 2007) with another triple *myb* mutant *myb75, myb90, and myb114* (Appelhagen et al. 2011) produced an *myb* sextuple mutant. This mutant was detected in the F2 generation through PCR analysis and studied for metabolite accumulation. However, seedlings of this mutant failed to accumulate flavonols or anthocyanins (Naik et al. 2021). The wild type (Col 0), *myb* sextuple mutants, and the corresponding *CaLAP*-overexpressing lines of *A. thaliana* were grown in the plant growth chamber (AR-41L3; Percival, Perry, IA, USA) with a photoperiod of 16-h light/8-h dark at 22 °C. *Nicotiana benthamiana* plants were grown in a plant growth chamber with an 8-h light/16-h dark photoperiod at 22 °C. The *A. thaliana* suspension cell culture At7 was derived from the hypocotyl of the reference accession Columbia (Col) and handled as described in Stracke et al. (2016).

Identification of the anthocyanin-specific transcriptional regulators from *C. arietinum*

The functionally characterized anthocyanin-specific R2R3-MYB transcriptional regulators from various plants were subjected to a tblastn search against the *C. arietinum* genome sequence for the identification of candidate anthocyanin-specific R2R3-MYB regulators in chickpea. The corresponding protein sequence of CaMYB was aligned with the previously characterized landmark MYBs (Rajput et al. 2022b) via MAFFT v.7.299b (Katoh and Standley 2013). The alignment was trimmed via phyx and finally subjected to MEGA X (Kumar et al. 2018) for the construction of a neighbor-joining phylogenetic tree with a 1000 bootstrap value.

Gene expression analysis

C. arietinum RNA-Seq data sets for 10-day-old samples (whole seedlings, seedling roots, seedling shoots, shoot apical meristem, developmental stages of seeds, germinating seedling, developmental stages of flower, reproductive plant, root, vegetative plants and young leaves) (BioProjects: PRJNA182724, PRJNA79731, PRJNA316844, PRJNA316845, SAMN00794551) (Garg et al. 2011; Rajkumar et al. 2020) were retrieved from the Sequence Read Archive (SRA, https://www.ncbi.nlm.nih.gov/sra). STAR v2.5.1b (Dobin et al. 2013) was applied to align the reads to the *C. arietinum* genome sequence in the two-pass mode. Reads were mapped if the alignment similarity exceeded 95% and covered 90% of the read length as previously described (Haak et al. 2018). Feature Counts v1.5.0-p3 (Liao et al. 2014) was deployed with default settings to quantify gene expressions. The resulting count tables were processed and combined by previously developed Python scripts (Haak et al. 2018). Heatmap construction was performed with HCE (Hierarchical Clustering Explorer 3.5), and the hierarchical clustering of genes was executed by the Euclidean distance method (Seo et al. 2006).

Total RNA from various tissues of chickpea was isolated from GSure plant RNA isolation kit (GCC Biotech, Kolkata, India). The isolated RNA was treated with RNAse-free DNAse (Thermo Fisher Scientific, Waltham, MA, USA). cDNA was synthesized using RevertAid H Minus First Strand cDNA Synthesis Kit (Thermo Fisher Scientific). The RTq-PCR analysis of selected genes was conducted using a 2 × PCR Master Mix (Applied Biosystems, Foster City, CA, USA). Each PCR mix contained 1 µl of diluted cDNA (equivalent to 25 ng total RNA), 5 µl of 2 × SYBR Green PCR Master Mix (Applied Biosystems), and 10 nM of each gene-specific primer in a final volume of 10 µl. All qRT-PCRs were done under the following conditions: 20 s at 95 °C, 3 s at 95 °C, and 40 cycles of 30 s at 60 °C in 384-well optical reaction plates (Applied Biosystems). The expression levels of various genes involved in anthocyanin and PA biosynthesis were assessed using the 7500 Fast Real-Time PCR System (Applied Biosystems). The integrity of the amplicons was confirmed by melting curve analysis conducted from 60 to 95 °C after 40 cycles. For normalization of transcript level, the housekeeping genes, chickpea *elongation factor 1-α* (*EF-1α*) (GenBank: AJ004960.1) and *Caβ-tubulin* (*Caβ-Tub*) (LOC101495306) coding sequence, were used. The cycle threshold (Ct) $2^{-\Delta\Delta CT}$ method was used to calculate the relation fold change (Livak and Schmittgen 2001). Three biological replicates and three technical replicates were used for mean value calculation. Primers used in the study are mentioned in Table S1.

Cloning of the transcription regulators from cDNA

The first-strand cDNA of *C. arietinum* cultivar ICC4958 was used as a template for amplifying the coding sequence of *CaLAP1*, *CaLAP2*, *CabHLH1,* and *CaTTG1*. The *C. arietinum* genome database sequence information was used to design the primers. The Gateway™ attB-site-containing primers and Gateway™ cloning vector pDONRTMZeo (Invitrogen) were utilized for the prepration of entry clones. All entry clones were subsequently confirmed by Sanger sequencing at the sequencing core facility of NIPGR (New Delhi, India).

Subcellular localization of CaLAPs

The coding sequence of CaLAP1 and CaLAP2 were recombined to CaMV35S promoter-driven C-terminal YFP in PGWB441 binary vector using Gateway™ LR-recombinase (Nakagawa et al. 2007).The resulting plasmids were transformed into *Agrobacterium tumefaciens* strain GV3101::pMP90 (Koncz and Schell 1986). The cultures and nuclear marker (NLS–RFP) were mixed with freshly prepared infiltration buffer (10 mM MES-KOH, pH 5.7, 10 mM $MgCl_2$, 150 µM acetosyringone) followed by co-infiltration in the leaves of 3-week-old plants of *N. benthamiana* and kept at 22 °C for 48 h. The infiltrated leaves were observed under a Leica TCS SP5 confocal laser-scanning microscope (Leica Microsystems, Wetzlar, Germany). RFP fluorescence was detected with excitation at 558 nm and emission at 583 nm, while YFP fluorescence was observed with excitation at 513 nm and emission at 530 nm.

Yeast two-hybrid (Y2H) assay

The entry clones of CaLAP1 and CaLAP2 were recombined in prey vector pGADT7g (Clontech Laboratories Inc., San Jose, CA, USA), and CabHLH1, CaTTG1 in the bait vector pGBKT7g (Clontech Laboratories Inc.). The Y2H Gold strain was initially cultured in yeast extract–peptone–dextrose (YPD) broth medium at 30 °C for 24 h. Following incubation, the culture was harvested by centrifugation at 3420 *g* for 5 min. The resulting pellet was then co-transformed by both prey and bait constructs plasmids into yeast gold strain using the EZ-yeast transformation kit (MP Biomedicals, Irvine, CA, USA) spread in SD/-Leu/-Trp (DDO, Double Dropout), lacking medium. The pGADT7g-CaLAP1, pGADT7g-CaLAP2, and pGBKT7g-CabHLH1, pGBKT7g-CaTTG1 containing yeast colonies were patched in SD/-Leu/-Trp (DDO, double dropout), SD/-Trp/-Leu/-His/-Ade (QDO, quadruple dropout), and 5 mM 3-amino-1,2,4-triazole (3-AT), X-α-gal -QDO plates and grown at 30 °C for 3 days. pGADT7-large with T/pGBKT7–53, and pGADT7-Iarge T/pGBKT7-Lamin combinations were used as a positive and negative control (Pipas and Levine 2001). Three repetitions of the experiment were performed, ensuring the inclusion of both positive and negative controls. Consistency in results was observed throughout.

Bimolecular fluorescence complementation (BiFC) assay

For BiFC assays, the entry clones of CaLAP1 and CaLAP2 coding sequences were recombined through LR clonase into the CaMV35S-driven vectors pSITE–YFP^N and CabHLH1, CaTTG1 into the pSITE–YFP^C (Martin et al. 2009). The resulting plasmids were transformed individually into *Agrobacterium tumefaciens* strain GV3101:pMP90 (Koncz and Schell 1986). *Agrobacterium* culture of both YFP^N and YFP^C fusion proteins construct was dissolved in freshly prepared infiltration medium (10 mM MES/KOH, pH 5.7, 10 mM $MgCl_2$, and 150 µM acetosyringone) and co-infiltrated (1:1 ratio) in leaves of 3-week-old *N. benthamiana*. The negative control set consisted of CaLAP1/2-pSITE–YFP^N with EV-pSITE–YFP^C and pSITE–YFP^N, alongside CabHLH1/CaTTG1-pSITE–YFP^C. After 48 h of incubation at 22 °C, YFP fluorescence (excited at 513 nm, emitted at 530 nm) was visualized using a Leica TCS SP5 laser-scanning confocal microscope at the NIPGR confocal facility. The experiment was repeated three times, with consistent positive and negative controls included each time. The results remained consistent across all three repetitions.

Luciferase complementation imaging (LCI) assay

For LCI, full-length CDS sequences of CaLAP1 and CaLAP2 entry clones were ligated in pCAMBIA1300-LUC^N and CabHLH1 in pCAMBIA1300-LUC^C (Chen et al. 2008). The resulting plasmids were transformed into *Agrobacterium tumefaciens* GV3101::pMP90 (Koncz and Schell 1986) and the cultures were individually suspended in infiltration medium (10 mM MES-KOH, pH 5.7, 10 mM $MgCl_2$,10 mM and 150 µM acetosyringone) and co-infiltrated in equal volume into *N. benthamiana* leaves. Luciferase substrate 100 µM D-luciferin was spread in infiltered *N. benthamiana* leaves after 48 h. A low-light charged-coupled device (CCD) imaging apparatus (Bio-Rad, Hercules, CA, USA) was used to quantify luciferase activity. The experiment utilized four *N. benthamiana* plants for each construct combination, with three repetitions performed. Results remained consistent with all repetitions.

Complementation analysis in *A. thaliana*

The entry clones of *CaLAP1* and *CaLAP2* were recombined using LR clonase into the destination vector pLEELA harboring 2 × 35S CaMV promoter and BASTA resistance for the selection. Resulting plasmids were transformed into *A. tumefaciens* strain GV3101::pM90RK (Koncz and Schell 1986) using electroporation. T-DNA insertion constructs containing *CaLAP1* and *CaLAP2* CDS were transformed into the *myb* sextuple *(myb12, myb111, myb11, myb75, myb90, myb114)* mutants of *A. thaliana* via *Agrobacterium*-mediated floral dip method (Clough and Bent 1998). BASTA-resistant *A. thaliana* seedlings were transferred to the soil-filled pots for further analysis.

Co-transfection analysis in *A. thaliana* At7 protoplasts

The co-transfection assay was performed using *A. thaliana* At7 protoplasts. The coding sequences of CaLAP1, CaLAP2, CabHLH1, and CaTTG1 were incorporated into the Gateway-compatible pBT-Dest destination vector, under the control of a 2 × 35S promoter, to generate the effector construct (Baudry et al. 2004). For the reporter constructs, entry clones having promoter sequences of *CaCHS6* and *CaDFR2* were recombined in the pDISCO destination vector. The cultivation of At7 cells, co-transfection of effector and reporter constructs into protoplasts, and the determination of activation capacity followed the methodology outlined in Stracke et al. (2010, 2016), Rajput et al. (2022b) and Saxena et al. (2023a, b).

Yeast one-hybrid (Y1H) assay

The Y1H assay was performed using the Y1H gold yeast strain (Takara Bio Inc., Shiga, Japan). The promoter fragments of *CaCHS* (1141 bp), *CaDFR2* (735 bp), *CaANS* (869 bp), and *CaANR* (1325 bp) were cloned into the pABAi vector (Cat. No. 630491, Takara Bio Inc.). The pABAi vector harboring promoter fragments was linearized with Bsp119I (BstBI) enzyme and transformed into Y1H Gold strain according to the Matchmaker™ manual. The CaLAP1 and CaLAP2 CDS fragments were also cloned into the pGADT7-gateway vector. The construct plasmids having the desired genes and empty pGADT7-gateway vector as control were transformed into pre-transformed Y1H strains containing target promoter sequence. The interactions were checked on Aureobasidin (AbA)-supplemented media. The growth of different promoter-integrated Y1H strains was checked under –Leu/SD media having different concentrations of AbA to determine the MIC (minimum inhibitory concentration) values.

Electrophoretic mobility shift assay (EMSA)

The electrophoretic mobility shift assay (EMSA) was performed using probes with biotin-labeled dUTP and the Light-Shift Chemiluminescent EMSA Kit (Thermo Scientific) as described previously (Xu et al. 2017). DNA fragments of *CaDFR2* promoter (53 bp) and *CaANS* promoter (48 bp) (Table S1) containing the CaLAP1/2-binding sequence were used. Both sense and antisense for the regular (WT) and mutated (MT) oligonucleotides were biotin labeled as described in the manual (biotin 3' end labeling kit). For bacterial protein expression, the specific primers (supplementary text Table S1) were used to amplify the CaLAP1-CDS and CaLAP2-CDS by using the clones of CaLAP1 and CaLAP2, respectively, and ligated at BamHI and HindIII restriction sites in pET28a + protein expression vector to express His-tagged proteins. His-tagged recombinant proteins expressed *E coli* BL21 (codon +) using the 0.5 mM IPTG and purified through Ni–NTA-beads.

Binding reaction for EMSA was set as described in the manual. Briefly, 1 µg His-tagged recombinant proteins containing 1 × binding buffer were incubated together with biotin-labeled probes in 20 µl reaction mixtures (containing 10 mM Tris–HCl, 150 mM KCl, 1 mM DTT, 50 ng/ml poly (dI-dC), 2.5% glycerol, 0.05% Nonidet P-40, 100 mM ZnCl2, and 0.5 µg/ml BSA) for 45 min at 25 °C and separated on 8% native polyacrylamide gels in 1 × TAE (Tris–acetate EDTA) buffer. The labeled probes were detected by using streptavidin–horse radish peroxidase (HRP) and chemiluminescence reagents according to the instructions provided with the EMSA kit. The figure legends provide information on the amount of protein (1 µg) for binding with the biotin-labeled probe (2 nM).

Dual-luciferase assay

The entry clones of *proCaANS* (1930 bp) and *proCaANR* (1816 bp) were recombined into the p635nRRF containing 35S:REN vector while entry clones of CaLAP1, CaLAP2, CabHLH1, and CaTTG1 were recombined into the PGWB420 destination vector (Ezquerro et al. 2023). These reporter and effector constructs were co-infiltered in different combinations in *N. benthamiana* leaves to determine the transactivation activity. Using the dual-luciferase reporter assay system (Promega, Madison, WI, USA), firefly luciferase and REN activity were assessed in the extracts of leaf discs after 48 h of co-infiltration, following the manufacturer's instructions. With the help of the POLAR star Omega multimode plate reader (BMG Labtech, Ortenberg, Germany), the samples were quantified, and the firefly luciferase activity was normalized to that of the REN. Four leaves of two plants were utilized for each combination of constructs, and the experiment was repeated twice. Consistency in results was observed across both repetitions.

Generation of transgenic chickpea lines

Transgenic chickpea lines were developed as described previously (Khandal et al. 2020; Pal et al. 2023; Saxena et al. 2023a, b). Briefly, chickpea (ICC4958) seeds were surface sterilized with ethanol and 2% sodium hypochlorite, followed by soaking for about 7–8 h. A healthy mature seed's half cotyledon and embryo were used as explant for agro-transformation of the construct of interest. The explant was incubated with the agro-suspended culture containing half-strength Murashige and Skoog (MS) medium (pH 5.5) and 100 µM acetosyringone for 30 min. The transformed explants were shifted to the half-strength MS plates for 48 h in the dark at 22 °C. Subculturing of these explants having radicle was done on the plates containing the shoot and root induction half-strength MS medium (pH 5.8) containing cefotaxime (250 mg/l) and kanamycin (200 mg/l). The healthy transformants were micro-grafted on the 7- to 10-day-old root stocks from the same accession. The acclimatization of these micro-grafted plants was done on a growth chamber (Conviron, Winnipeg, Canada) at 22–24 °C with 60% humidity and a 10-h light period with an intensity of 250 µmol m^{-2} s^{-1} to maturity.

Total anthocyanin quantification

Total anthocyanin content was quantified using the spectrophotometric method as described previously (Pandey et al. 2014, 2015). Briefly, 2.5 ml of acidic methanol (1%, v/v) was added to 0.25 gm of lyophilized fine ground tissue, and the extract was incubated overnight at 4°C in the dark. The mixture-lysate was centrifuged at 3000 *g*, the supernatant was collected, and absorbance was measured at 530 and 657 nm. The anthocyanins were quantified using the formula: (A_{530}–0.25 × A_{657})/tissue weight.

Total PA quantification

The seed coat of wild-type (ICC4958) and *CaLAP1-2*-OE lines was used for the extraction and quantification of soluble and insoluble PA as mentioned in Pang et al. (2007). For estimating the PA content in samples, different dilutions of catechin were used to develop the standard calibration curve (200, 400, 600, 800, and 1000 µg/ml).

Lyophilized seed coat samples were powdered and added with 1 ml of extraction buffer (butanol–HCl reagent (5:95, v/v) containing 0.7 g $FeCl_3$/l) and vortexed, followed by sonication. The sonicated extract was filtered with 0.22 µm PVDF filters (Merck Millipore, Darmstadt, Germany). The absorbance was measured at 550 nm following a 1 h boil to determine the insoluble PA content. Samples were cooled to room temperature, and the absorbance was measured again at 550 nm. A standard curve of procyanidin B1 (Merck) at dilutions of 50, 100, 150, 200, and 250 µg/ml was developed to estimate PA content in the samples.

UHPLC and LCMS analysis of chickpea seed tissue

Monomeric and oligomeric PAs were estimated in three biological and three technical replicates, following the methodology described previously (Rajput et al. 2022b; Pal et al. 2023).. Lyophilized seed coat and embryo tissue samples (200 mg) were extracted with 80% methanol. The clear supernatant extract was filtered through 0.22 µm for analysis. Three volumes of 2 M acidic methanol:HCl were added and incubated for 45 min at 90 °C. The samples were dried in rotavapor and resuspended in 1 mL 80% methanol. The analysis was performed using a 1290 Infinity II series UHPLC system (Agilent 290 Technologies, Santa Clara, CA, USA) enabled with a Zorbax Eclipse Plus C18 column kept at 30 °C. The mobile phase composition was solution A (0.1% formic acid in HPLC-grade water) and solution B (0.1% formic acid in acetonitrile). However, the chromatographic parameters included a constant flow of 270 µl/min (injection volume, 3 µl) and a run time of 47 min, including equilibration time. Before analysis, all samples were sterilized using a 0.22 µm PVDF syringe filter (Merck). For the anthocyanin quantification, we used the LC–MS systems. A UHPLC system (Exion LC Sciex, Framingham, MA, USA) connected to a triple quadrupole (QTRAP6500 +) (ABSciex, Framingham, MA, USA) using electrospray ionization was used to analyze the PAs. The positive ionization voltage was set at 5500 V. Utilizing the Analyst software (version 1.5.2), the mass spectrometer was used in a variety of reaction monitoring modes for both qualitative and quantitative analysis. Analytical standards (Merck) were used for each compound.

Statistical significance

We utilized one-way ANOVA followed by Tukey's post hoc test to compare multiple datasets ($*P \leq 0.05$; $**P \leq 0.01$; $***P \leq 0.001$, $****P \leq 0.0001$). Each dataset comprised three replicates.

Results

Identification of anthocyanin-specific R2R3-MYB regulators from *C. arietinum*

In our previous study, an in silico analysis led to the identification of 119 putative R2R3-MYB regulators in chickpea (Rajput et al. 2022b). Here, we identified two homologs of

R2R3-MYB activators, CaLAP1 (CaMYB16) and CaLAP2 (CaMYB30), exhibiting high similarity to the known anthocyanin regulators associated with legume anthocyanin production (LAP). *CaLAP1* and *CaLAP2* encode the proteins comprising 250 and 236 amino acids, respectively. The phylogenetic study showed the clustering of CaLAP1 and CaLAP2 with the previously characterized anthocyanin-specific R2R3-MYBs (Fig. 1a). The amino acid alignment revealed that CaLAP proteins share a highly conserved N-terminal R2R3-MYB domain having COP1-interacting VP motif (VP [E/D] RAG), bHLH-interacting consensus motif ([D/E] Lx2[R/K]x3Lx6Lx3R) and dicot-specific conserved ANDV motif that distinguishes it from the monocot-specific DNEI motif. Additionally, the C-terminal region contains an anthocyanin-specific SG6 motif (KPRPR [S/T] F) (Fig. 1b).

CaLAP proteins are nuclear localized

The subcellular localization of CaLAP proteins was confirmed by transient expression of gene constructs encoding CaLAP proteins fused to yellow fluorescent protein (YFP) and a nuclear marker red fluorescence protein (RFP) fused to a nuclear localization signal (NLS–RFP) in *N. benthamiana*

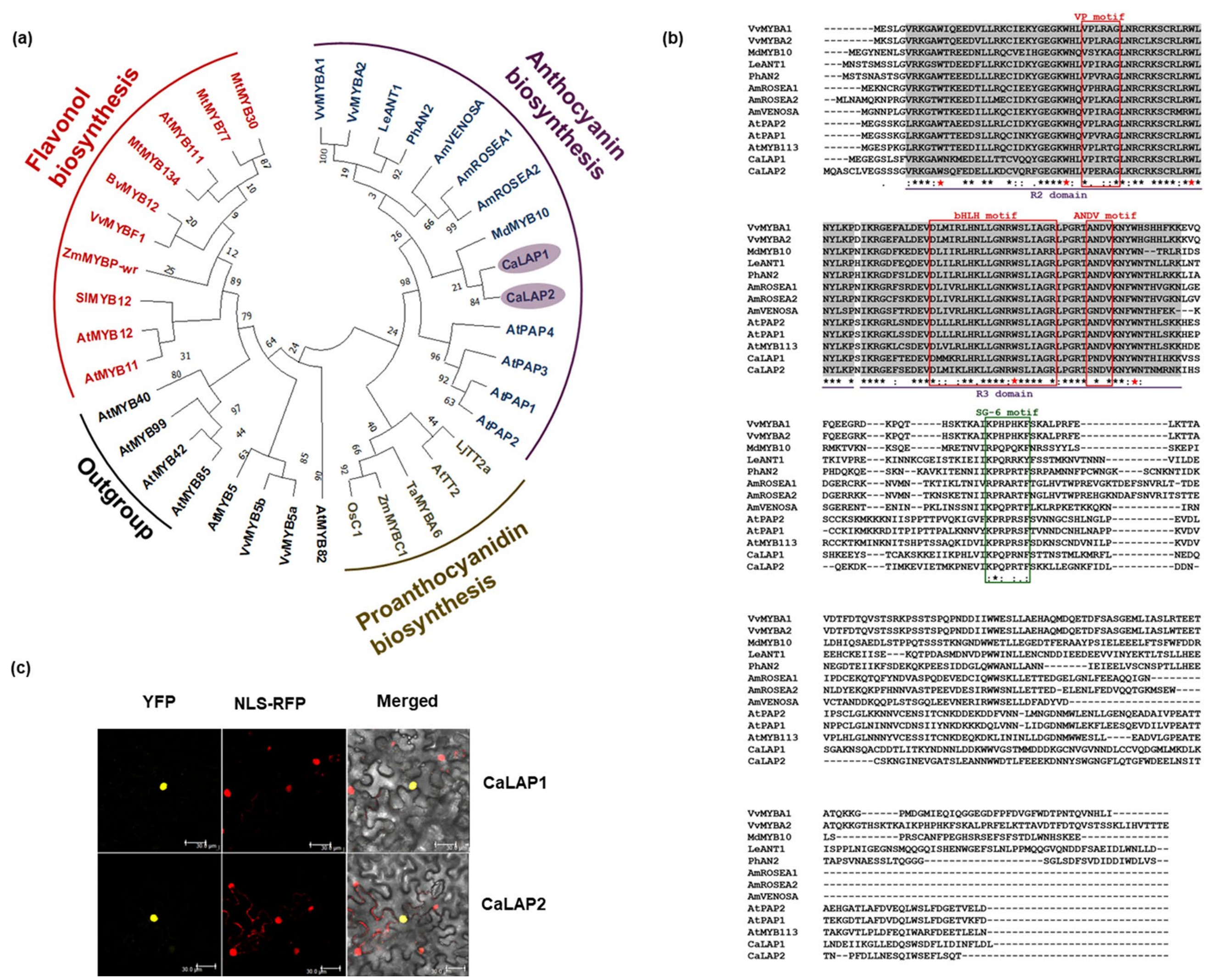

Fig. 1 Phylogenetic analysis, amino acid sequence alignment, and sub-cellular localization of candidate anthocyanin-specific R2R3MYB proteins in chickpea genome. **a** The depicted R2R3-MYB proteins were classified into three major groups: flavanol, anthocyanin, and proanthocyanidin biosynthesis-specific regulators using landmark flavonoid-specific R2R3-MYBs from different plant species. The phylogenetic tree was constructed using MEGA X. CaLAP1 and CaLAP2 are highlighted by purple ovals. **b** The R2 and R3 repeat within the MYB domain, alongside the bHLH interaction motif and the S6 defining motif, are annotated based on known anthocyanin-specific R2R3-MYB regulators. The VP domain, representing the COP1-interacting domain, is identified within the MYB R2 domain. **c** Subcellular localization of CaLAP–YFP fusion proteins in *Agrobacterium*-infiltrated tobacco leaves analyzed by confocal microscopy. NLS–RFP was used as a nuclear marker

leaves. CaLAP1–YFP and CaLAP2–YFP fusion proteins were expressed exclusively in the nucleus and co-localized with the nuclear marker NLS–RFP suggesting that CaLAP1 and CaLAP2 are nuclear proteins (Fig. 1c).

The expression patterns of *CaLAP* correlate with putative structural target gene expression

We conducted an analysis using a publicly available RNA-Seq dataset comprising different tissues and developmental stages of seeds and flowers to analyze the expression of *CaLAP1* and *CaLAP2*, along with *CabHLH1* and *CaTTG1* involved in the MBW complex formation and anthocyanin and PA biosynthesis enzymes coding genes. *CaLAP1* expression was abundant in root and early developmental stages of seeds (S1–S4) and found in varying levels in different stages of flowers, whereas a very low expression of *CaLAP2* was observed in the early developmental stages of seeds (S1–S4). The expression levels of *CaANR* and *CaLAR* were notably elevated during the seed developmental stages, particularly at stage 6 and stage 7, while showing varying expression levels in other tissues. *CabHLH1* expression was higher at all stages of seed development and flowers, while *CaTTG1* expression was constitutive and abundant in all tissues. Likewise, the expression of the putative anthocyanin biosynthesis genes, *CaDFR2* and *CaANS*, showed a strong correlation with regulatory gene expression (Fig. 2a). The RT-qPCR data revealed a significantly higher expression

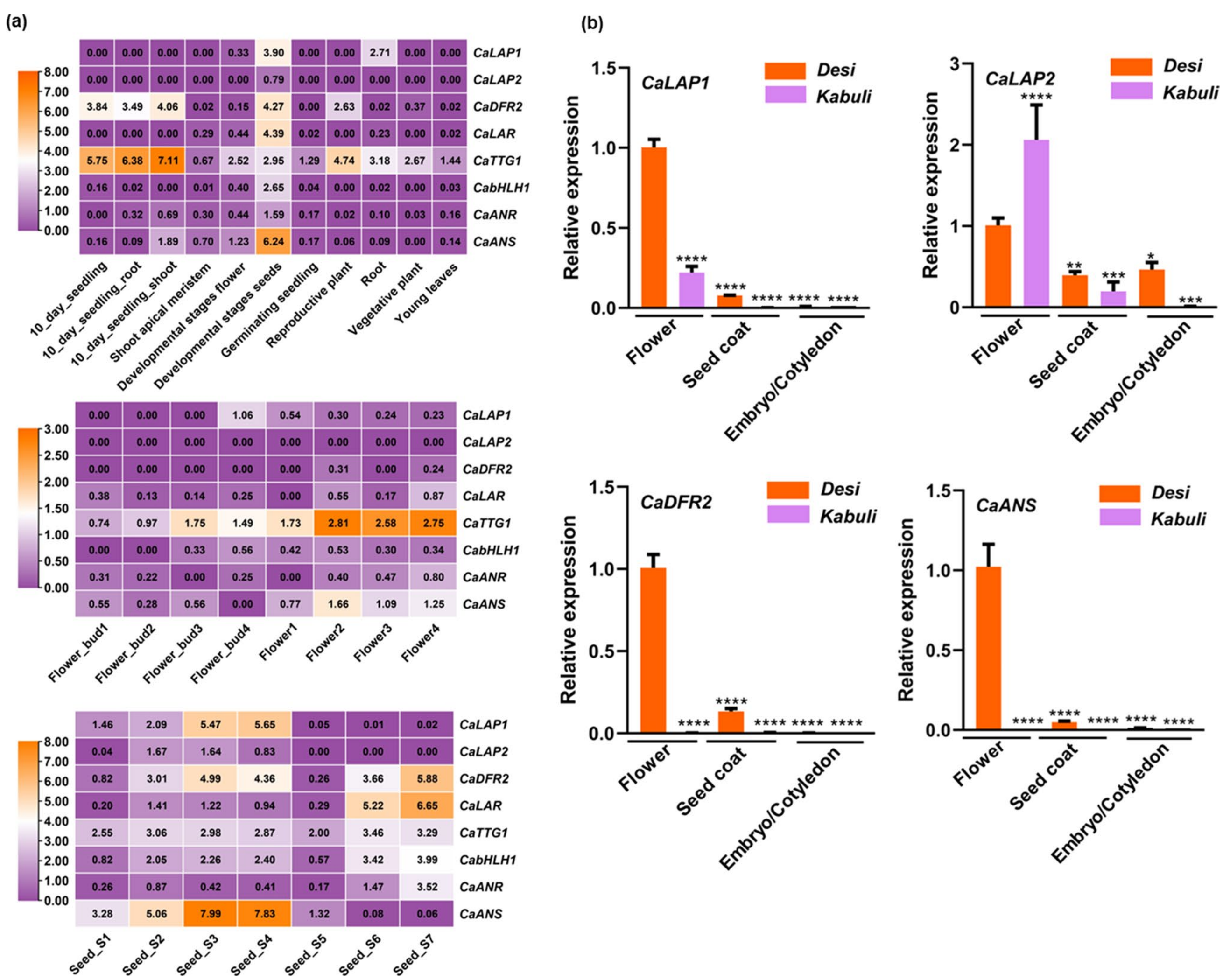

Fig. 2 Expression analysis of regulatory and structural biosynthesis genes in two *Cicer arietinum* cultivars with different flower and seed coat colors. **a** Differential expressions of regulatory genes (*CaLAP1, CaLAP2, CabHLH1, CaTTG1)* and structural biosynthesis genes (*CaDFR*2, *CaANS CaANR, CaLAR*) were calculated from publicly available RNA-Seq data sets of various plant parts and developmental stages of flowers and seeds. **b** Expression of *CaLAP, CaDFR2* and *CaANS* genes in flower and mature seed coat and embryo/cotyledon. The presented RT-qPCR data cover two independent biological replicates with three technical replicates of each and the error bars give ± SD values. *CaEF-1α* and *CaβTub* expressions were used as a reference control

of *CaLAP1, CaDFR2,* and *CaANS* genes in flower tissue as compared to seed coat and cotyledon in the *Desi type*. Conversely, *CaLAP2* expression was notably elevated in the *Kabuli type* cultivar (Fig. 2b). A robust correlation was identified between the expression levels of the candidate *CaLAP1* genes and *CaANS, CaDFR2, CaANR,* and *CaLAR,* particularly with higher expression observed in the seed coat. In contrast, *CaLAP2* exhibited lower expression in the seed coat despite overlapping expression patterns. These findings suggest that the R2R3-MYB (CaLAP1 and CaLAP2) may function as positive regulators of anthocyanin biosynthesis in chickpea.

CaLAP1 and *CaLAP2* partially restore the anthocyanin-deficient phenotype of the *A. thaliana myb* mutant

Anthocyanin-deficient *myb* sextuple mutant (Naik et al. 2021) was used to assess the *in planta* function of *CaLAP1* and *CaLAP2* as anthocyanin regulators under the control of the CaMV35S promoter. Transgenic seeds were grown on the half-strength MS medium supplemented with 4% sucrose. The accumulation of anthocyanin was observed in seedlings of Col 0 (wild-type control), which turned dark purple, whereas the *myb* mutant seedlings showed no anthocyanin accumulation. However, seedlings of transgenic *myb* mutant lines bearing the *35S::CaLAP1* and *35S::CaLAP2* constructs showed a light purple color, indicating partial accumulation of anthocyanin (Fig. S1). These results suggested that *CaLAP1* and *CaLAP2* have the potential to partially complement the anthocyanin deficiency phenotype of *myb* sextuple mutants of *A. thaliana*.

CaLAP1 and CaLAP2 interact with CabHLH1 and CaTTG1

Since CaLAP1 and CaLAP2 both contain a bHLH-binding motif ([DE]Lx2[RK]x3Lx6Lx3R) and anthocyanin biosynthesis depends on the formation of a regulatory MBW complex, we tested the potential interaction of these proteins with CabHLH1 and CaTTG1 co-factor. We selected our previously characterized chickpea bHLH1 protein (Rajput et al. 2022b; Pal et al. 2023) as a candidate to analyze the interaction with CaLAP1 and CaLAP2. The Y2H results indicate that both CaLAP1 and CaLAP2 interact with CabHLH1 (Fig. 3a). To validate the results *in planta*, we performed BiFC and LCI assay. In BiFC assay, reconstruction of YFP fluorescence was detected when CaLAP1–YFP^N or CaLAP2–YFP^N with CabHLH1–YFP^C pairs were transiently expressed in *N. benthamiana* leaves (Fig. 3b). LCI assay further confirmed the interactions by showing luminescence signal between the CaLAP1–CabHLH1 and CaLAP2–CabHLH1 pairs (Fig. 3c). Since a functional MBW complex needed a WD40-repeat protein, we also tested the interaction of CaLAP1 and CaLAP2 with CaTTG1. Y2H results confirmed interactions between both CaLAP1 and CaLAP2 with CaTTG1. The *in planta* interaction was also validated through BiFC assays (Fig. S2). This supports the hypothesis that these proteins may play a significant role in anthocyanin regulation through participation in MBW complexes.

CaLAP proteins form functional MBW complexes to activate anthocyanin and PA biosynthetic gene promoters

To establish connections between TFs and their targets, we conducted an analysis focusing on putative MYB-binding sites (MBS) within the promoters of genes involved in anthocyanin and PA biosynthesis. Initially, we examined the promoters of *CaCHS6*, *CaDFR2*, *CaANS*, and *CaANR* to identify potential MBSs. Structural analysis of the promoter regions, upstream of the transcription start site, identified several potential MBS motifs.To further extend the target specificities of CaLAP1 and CaLAP2 toward anthocyanin biosynthesis gene promoters, we performed PEG-mediated transient transfection in *A. thaliana* protoplasts. MBW complex-forming R2R3-MYB proteins CaLAP1, and CaLAP2, along with CabHLH1 and CaTTG1, were used in combination as effector constructs, while *proCaCHS6* and *proCaDFR2* were the reporter constructs. The co-transfection analyses suggested that CaLAP1 and CaLAP2 alone transactivate *proCaCHS6* and *proCaDFR2* to some extent, while in combination with CabHLH1 and CaTTG1 further enhanced the transactivation of *proCaCHS6* and *proCaDFR2* considerably (Fig. 4a). We also tested the potential of CaLAP1 and CaLAP2 in combination with AtEGL3 effector constructs in an At7 protoplast using *proAtLDOX, proAtDFR*, and *proAtCHS* reporter constructs that were assayed for their activity under the control of the CaMV35S promoter. We found the weak regulatory activity of CaLAP1 and CaLAP2 as compared to AtPAP1 effectors to activate anthocyanin biosynthesis in vivo in a heterologous system (Fig. S3).

To test the physical interactions between CaLAP1 and CaLAP2 with the promoters of *CaCHS6*, *CaDFR2*, *CaANS*, and *CaANR*, Y1H was conducted. *proCaCHS6* and *proCaDFR2* were found to harbor two MYB-binding sites each, while *proCaANS* possessed two MBS sites and one MYB-CORE site, and *proCaANR* featured three MYB-binding sites (Fig. S4). Both CaLAP1 and CaLAP2 exhibited binding affinity toward *proCHS6-1325, proCaDFR*-735, *proCaANS*-869, and *proCaANR-1141*. Conversely, the respective empty vector controls did not display such interactions. These findings suggest that *proCaCHS6, proCaDFR2, proCaANS,* and *proCaANR* are probable target genes of both CaLAP1 and CaLAP2 (Fig. 4b). Additionally, to know about the direct binding of CaLAP1 and CaLAP2 transcription

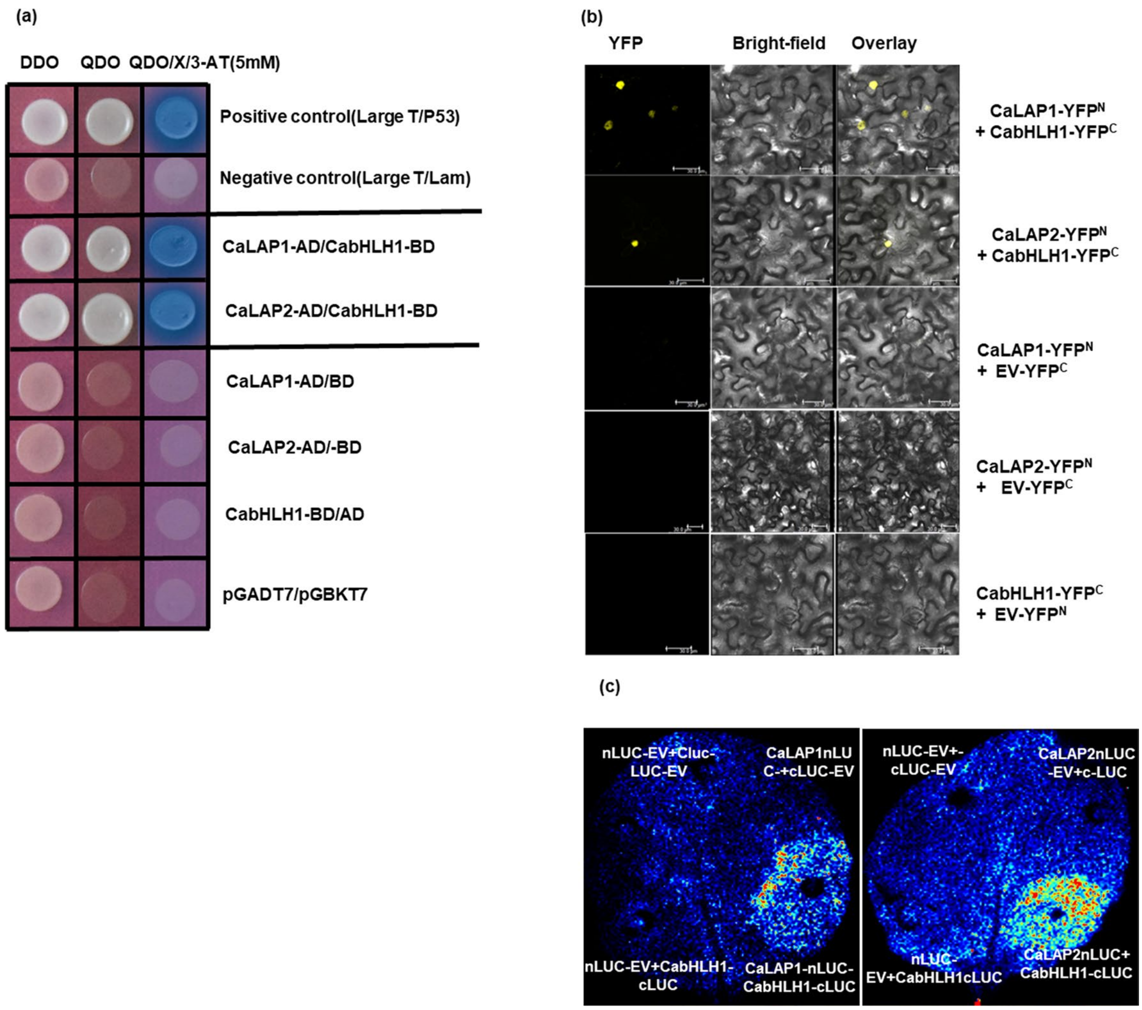

Fig. 3 CaLAP1 and CaLAP2 interact with CabHLH1 as a part of the functional MBW complex. **a** Yeast two-hybrid (Y2H) assays showed in vivo interaction between CaLAP1 and CaLAP2 proteins with CabHLH1. AD, Gal4 activation domain; BD, Gal4 DNA-binding domain; DDO, double synthetic dropout (SD)-Leu-Trp medium; QDO/X, quadruple SD-Leu-Trp-Ade-His + X-α-Gal. **b** Bimolecular fluorescence complementation (BiFC) assay indicates planta interaction of CaLAP1, CaLAP2 with CabHLH1. Scale bar = 20 µm. **c** Luciferase complementation imaging (LCI) assay showing the interaction between CaLAP1 and CabHLH1 and CaLAP2 and CabHLH1

factors on *proCaDFR2* and *proCaANS*, we performed gel-shift assay (EMSA). We found that the sequences TAACCT for *proCaANS* and TAACAG for *proCaDFR2* are the sites at which CaLAP1 and CaLAP2 bind (Fig. 4c and Table S1).

Further, to assess the transactivation activity of the effectors on the promoters of *CaANS* and *CaANR* genes, dual-luciferase assays were performed in *N. benthamiana* leaves. Reporter constructs were co-infiltrated with the effector constructs in the following combinations: CaLAP1 and CaLAP2 individually, CaLAP1 and CaLAP2 separately with CabHLH1, and the combination with both CabHLH1 and CaTTG1. Interestingly, both reporter constructs, pro*CaANS* and pro*CaANR*, exhibited less transactivation activity with effectors CaLAP1 and CaLAP2 individually. However, the transactivation activity drastically increased when CabHLH1 was also present. The promoter of *CaANS* and *CaANR* showed the highest transactivation activity in the presence of all three effector constructs including CaLAP1 or CaLAP2, CabHLH1, and CaTTG1, suggesting a synergistic role in activating the promoters of *CaANS* and *CaANR* (Fig. 4d).

CaLAP1 and CaLAP2 modulate total anthocyanin and PA contents in chickpea seed coat

The chickpea transgenic lines overexpressing *CaLAP1* and *CaLAP2* under the control of CaMV35S promoter were found

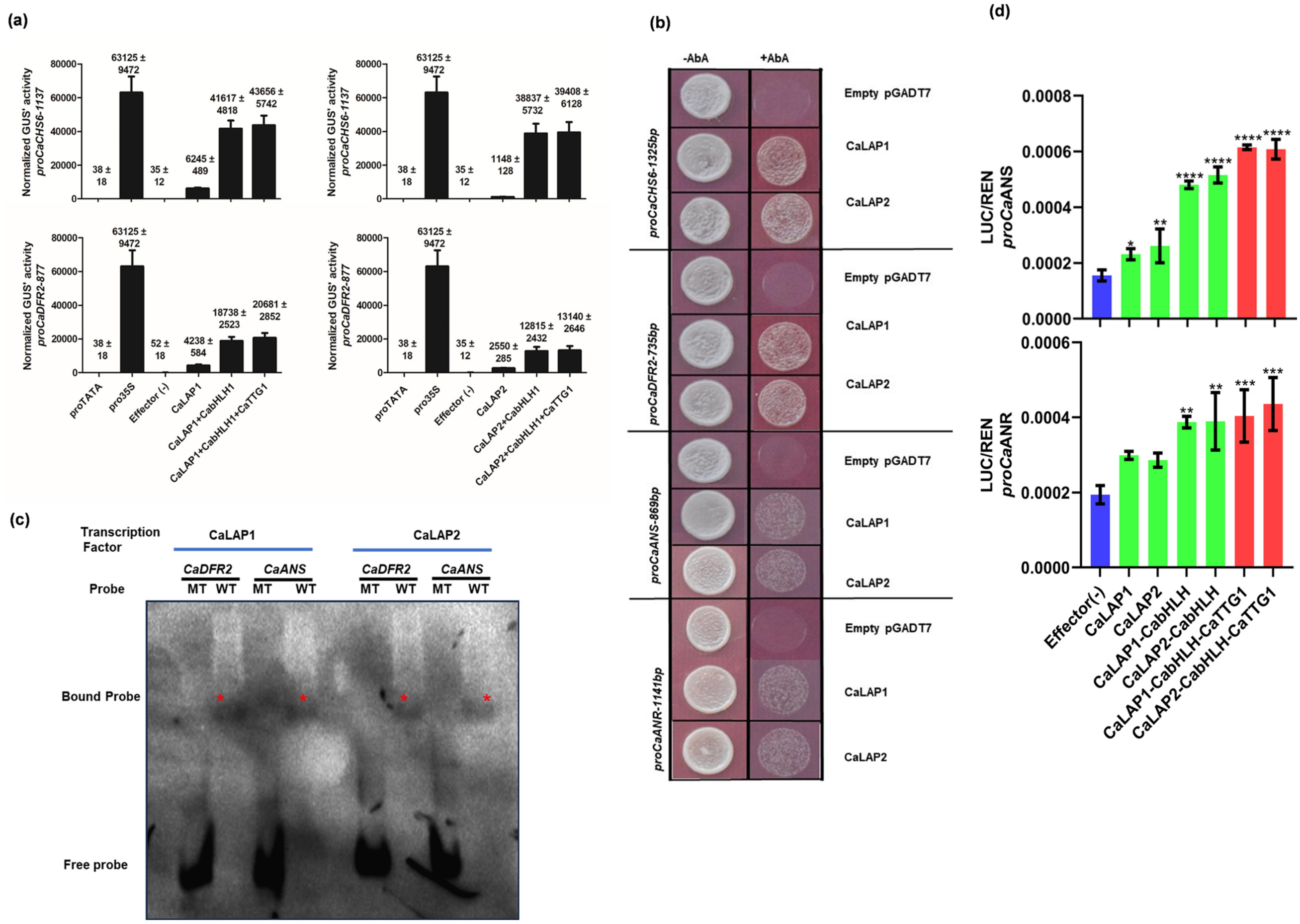

Fig. 4 CaLAP1 and CaLAP2 form an MYB–bHLH–WD40 (MBW) complex, which transactivates and binds to the promoters of genes involved in anthocyanin and proanthocyanin biosynthesis. **a** Results from co-transfection experiments in *Arabidopsis* protoplasts. Reporter constructs consisting of GUS driven by 1137-bp *CaCHS6* and 877-bp *CaDFR2* promoter fragments (reporter) were assayed for their transactivation by the 35S promoter-driven effectors CaLAP1, CaLAP2, CabHLH1, and CaTTG1, either alone or in the indicated combinations. Data are shown as the means of normalized GUS activity. **b** Yeast 1-hybrid assay. CaLAP1 and CaLAP2 physically interact with the promoters of *CaCHS6, CaDFR2, CaANS,* and *CaANR*. The physical interaction between CaLAP1, CaLAP2, and the *proCaCHS6, proCaDFR2, proCaANS,* and *proCaANR* was examined on leucine dropout media (-Leu) supplemented with an appropriate concentration of Aureobasidin (AbA). Strains transformed with the pGADT7 vector served as negative controls. The minimum inhibitory concentration (MIC) value for *proCaCHS6* and *proCaANR* was determined to be 900 ng/ml AbA, while it was 800 ng/ml for *proCaANS* and 600 ng/ml for *proCaDFR2*. **c** Gel-shift assay (EMSA) using a 53-bp region of *CaDFR2* promoter and 48-bp region of *CaANS* promoter surrounding the putative binding sequences and CaLAP1 and CaLAP2 proteins. Each lane has 5 nM of biotin-labeled DNA probe and protein with either mutated probe (MT) or wild-type (WT) probe and CaLAP1 or CaLAP2 protein with 1 µg concentration. **d** Dual-luciferase experiments were performed transiently in *Nicotiana benthamiana* leaves. Constructs harboring the firefly luciferase reporter gene (LUC) are driven by *CaANS-1930 bp,* and *CaANR-1816 bp* promoter fragments and were transiently co-infiltrated with CaLAP1, CaLAP2, CabHLH1, and CaTTG1 effector constructs, either alone or in the mentioned combinations. Data are presented of four biological and two technical replicates with ± SD

to be morphologically similar to the control plants except for the seed pigmentation, which was darker in the overexpressing lines (Fig. 5a). To assess the changes in the the metabolite content in *CaLAP*-overexpressing lines, we performed the spectrometric quantification of total anthocyanin and PA content (Fig. 5b and c). The analysis showed significantly higher anthocyanin and PA content in the seed coat of overexpressing lines than in the control lines suggesting that the overexpression of *CaLAP1* and *CaLAP2* enhances the biosynthesis of these pigments in chickpea.

CaLAP1 and CaLAP2 induce expression of the anthocyanin and PA biosynthetic genes in chickpea

Next, we performed gene expression analysis of regulatory and biosynthetic genes in the seedcoat of immature green seeds and the same embryo/cotyledon tissue of independent (L1, L2, and L3) chickpea *CaLAP1*-OE and *CaLAP2*-OE lines. In the overexpressing lines of *CaLAP1*, the *CaLAP1* gene expression showed a 10-fold increase in the seed coat

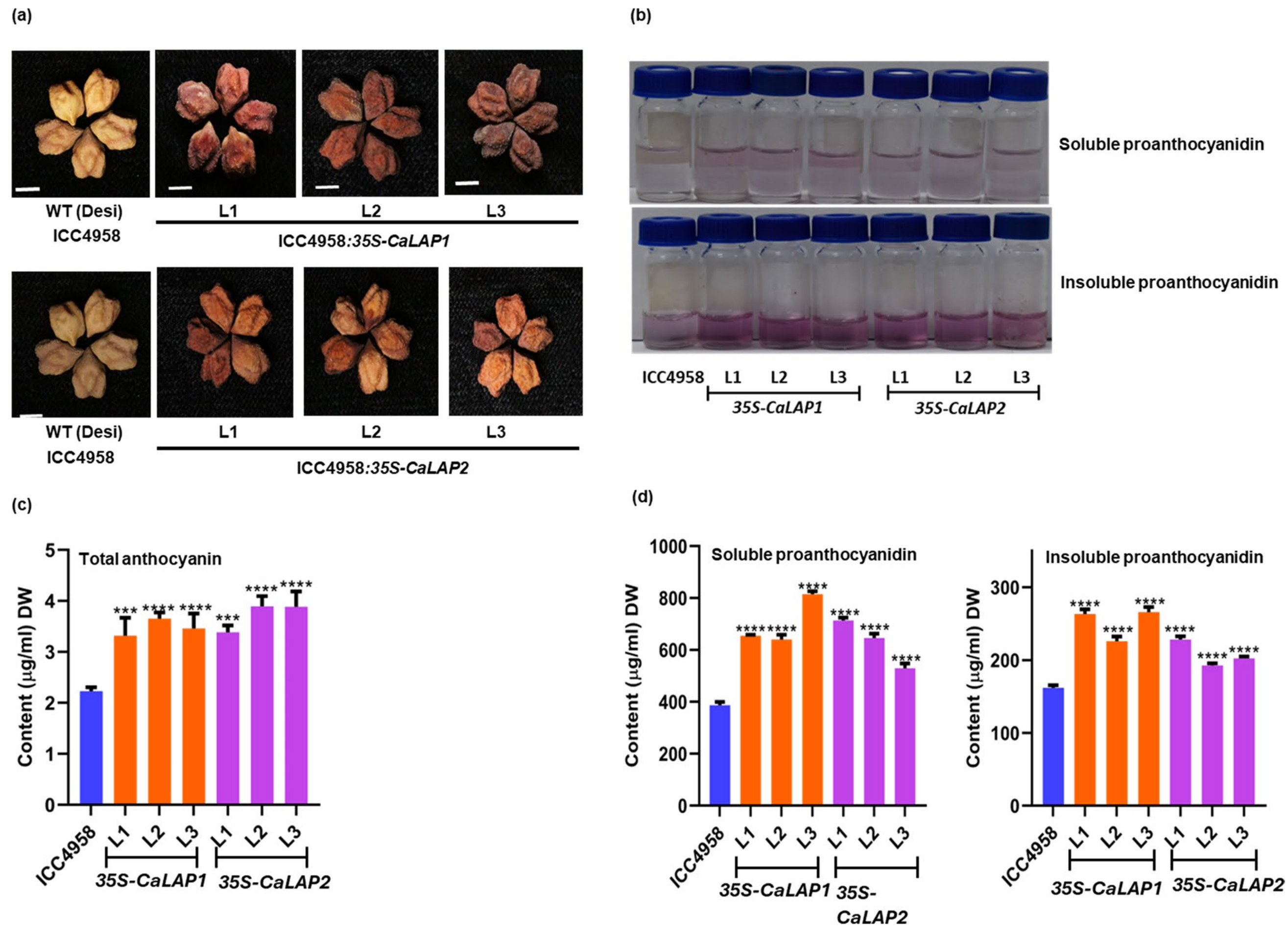

Fig. 5 *CaLAP1* and *CaLAP2* overexpression induces anthocyanin and PAs accumulation in the seed coat of *C. arietinum. a* Phenotype showing a clear distinction in the seed pigmentation due to overaccumulation of anthocyanins and PAs in the *CaLAPs*-OE lines of *C. arietinum.* **b** Representative visuals indicating the content of both soluble and insoluble PAs. **c** Total anthocyanincontent was determined using a spectrophotometer in both ICC4958 control chickpea lines and *CaLAP1* and *CaLAP2* overexpressing lines. **d** Soluble PAs were quantified using the DMACA reagent with catechin as the standard for absolute quantification. Insoluble PAs were estimated from dried seed tissue using the butanol–HCl reagent, with procyanidin B1 as the standard for absolute quantification in both control and transgenic seeds. The transgenic lines exhibited elevated levels of total anthocyanin accumulation and total PAs (soluble and insoluble). The values represent the means ± standard deviations of two biological replicates, with three technical replicates each for control and overexpressing lines

and 2–4-fold in the embryo/cotyledon, while *CaLAP2* expression displayed up to 10- to 22-fold upregulation in seed coat tissue and 2–3-fold in embryo/cotyledon in the *CaLAP2* overexpressing lines as compared to the control lines. The transcript levels of *CaDFR* and *CaANS* were elevated by 2- to 4-fold in the seed coat, while *CaANR* and *CaLAR* exhibited upregulation by 2- to 4- and 4- to 6-fold, respectively, in seed coat tissue compared to the control line. Similarly, *CaLAR* and *CaANR* also showed increased expression (Fig. 6a). Additionally, enhanced expression of *CaDFR, CaANS, CaANR,* and *CaLAR* was observed in embryo/cotyledon tissues of the same transgenic lines (Fig. 6b).

CaLAP1 and CaLAP2 modulate derivatives of anthocyanin and PA contents in the chickpea seed coat

To further substantiate our findings, we measured the anthocyanidin and PA content through LC–MS in the seed coat tissue of control and *CaLAP*1 and *CaLAP2* overexpressing lines of chickpea. Three anthocyanidins, cyanidin, delphinidin, and petunidin, accumulated in higher amounts (up to 4-fold) in overexpressing lines as compared to the control seed coat tissues of chickpea (Fig. 7a). In addition, monomeric PAs such as catechin, epigallocatechin, epicatechin gallate, as well as oligomeric PAs procyanidin A1, B2 and C1 were found to be significantly increased in the overexpressing lines as compared to the control plants (Fig. 7b and

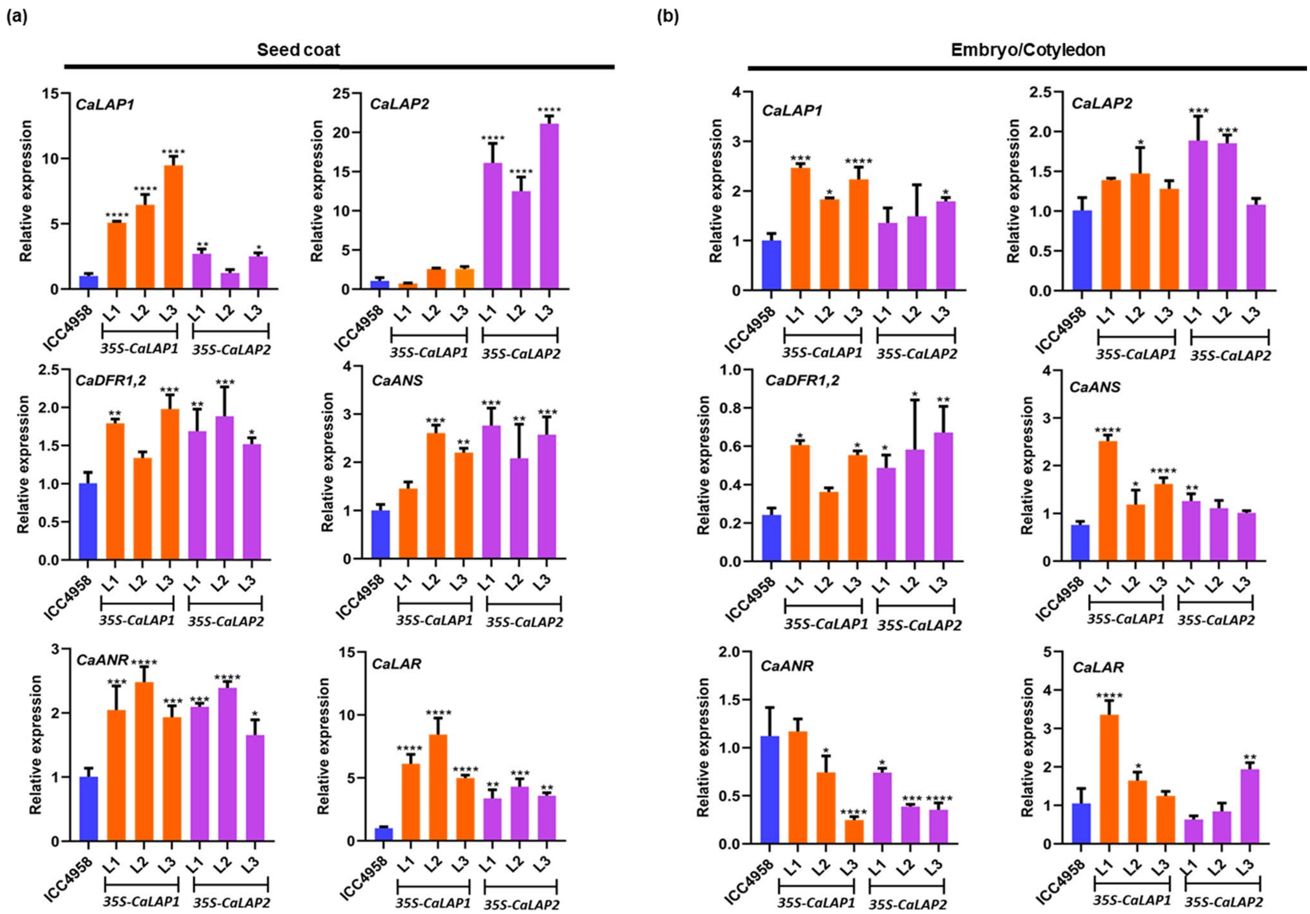

Fig. 6 Expression analysis of anthocyanin regulators and biosynthetic genes in control and *CaLAP1* and *CaLAP2* overexpressing lines of seed coat and cotyledon tissue of *C. arietinum*. **a** Differential gene expressions of *CaLAP1, CaLAP2, CaDFR1&2, CaANS*, and *CaANR* show significantly higher transcript in Ca*LAP1* and Ca*LAP2*-OE lines as compared to the ICC4958 control seed coat tissue. **b** Differential gene expressions of *CaLAP1, CaLAP2, CaDFR1&2, CaANS*, and *CaANR* show higher transcript values in a few lines of *CaLAP1* and *CaLAP2*-OE lines as compared to ICC4958 control in embryo cotyledon tissue. The RT-qPCR data cover three technical triplicates, and the error bars give ± SD values. The expression level in control was set as 1 and relative expression levels are given. CaEF-1α expression was used as the reference control

c). These findings suggest the role of *CaLAP1* and *CaLAP2* in regulating pigment production in chickpea.

Discussion

Chickpea seeds are well known for their high contents of protein, antioxidants, and flavonoids, including anthocyanin and PA (Jameel et al. 2021; Rajput et al. 2022b; Grasso et al. 2022; Saxena et al. 2023a, b). Using a transgenic approach, targeting biosynthetic genes and regulatory proteins hold significant potential for enhancing the flavonoid content in chickpea. The flower and seed colors are among the earliest phenotypic traits studied in plant genetics and inheritance. Several anthocyanin derivatives, including cyanidin, malvidin, petunidin, pelargonidin, delphinidin, and peonidin, have been shown to aggregate in the chickpea seeds, conferring brown color to the seed coat in Desi chickpea (Pal et al. 2023). The rough texture and astringent flavor are attributed to the presence of PAs derivatives (catechin, epigallocatechin, and epicatechin gallate) in the chickpea seed coat (Soares et al. 2020). In our earlier investigation, it was observed that the RNAi knockdown lines of TT8-like CabHLH and multidrug and toxic compound extrusion (CaMATE) exhibited reduced levels of anthocyanin and PA derivatives in both flower and seed coats (Pal et al. 2023). Rajput et al. (2022b) characterized the PA-specific TFs, CaPAR1 and CaPAR2 TFs, providing insights into the complex regulation of PAs in chickpea.

The transcript levels of anthocyanin-associated biosynthesis genes, such as *CaDFR* and *CaANS,* which were notably elevated during flower and seed development stages, exhibited a significant correlation with the expression of *CaLAP1*, indicating its regulatory role in reproductive

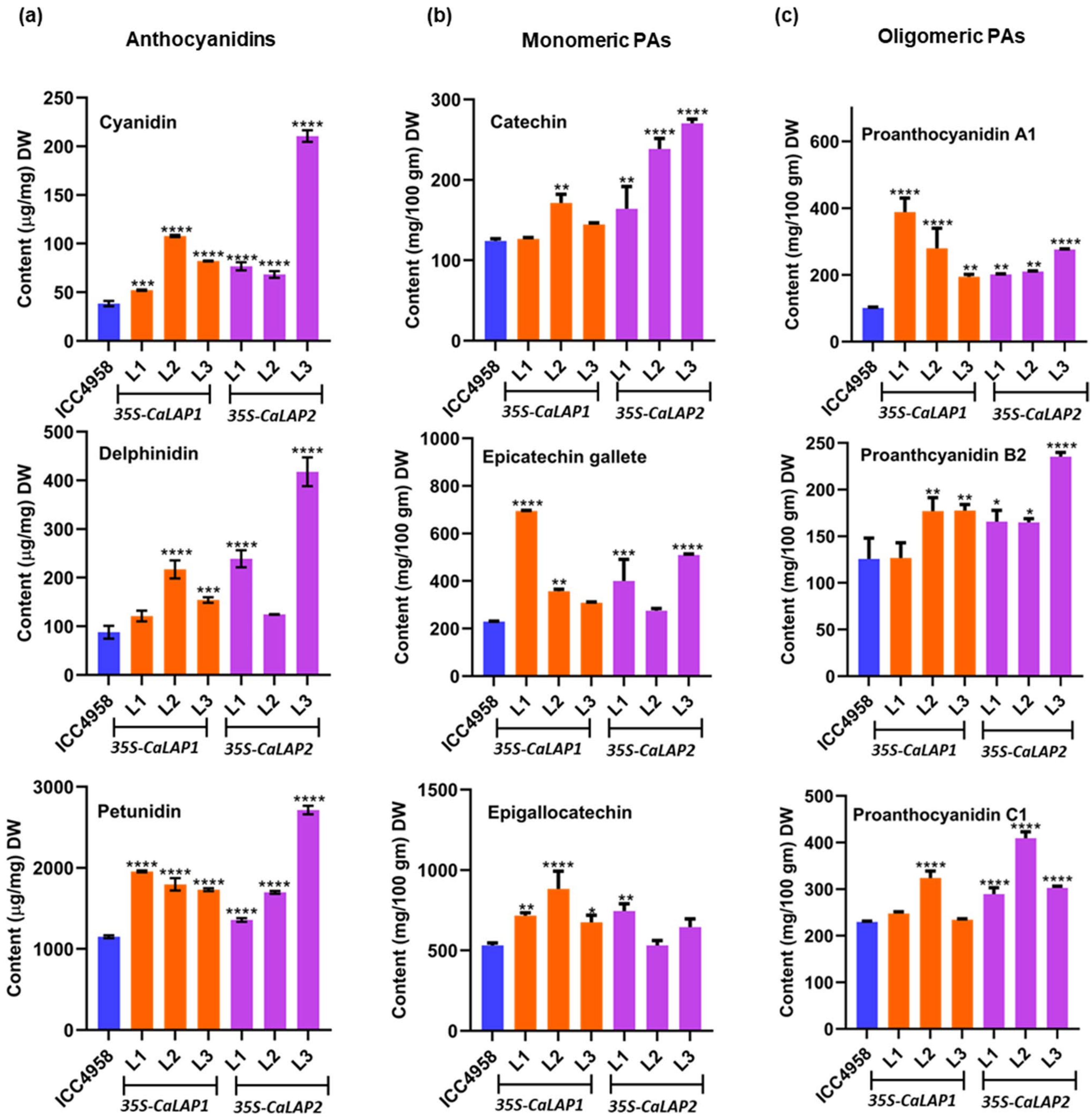

Fig. 7 Targeted metabolite profiling for quantitative estimation of anthocyanins and PAs in the control and transgenic lines of *C. arietinum. a* Estimation of anthocyanin derivatives (cyanidin, delphinidin, petunidin) in the control (ICC4958) and *CaLAP1* and *CaAP2*-OE lines. Anthocyanin derivatives in seed coat tissues of the control (ICC4958) and *CaLAPs*-OE lines by LC–MS analysis. **b** Monomeric forms of PAs: catechin, epigallocatechin, and epigallocatechin. **c** Oligomeric PAs: procyanidin A1 and procyanidin B2 and procyanidin C1. The monomeric and oligomeric forms of PAs were estimated using ultra-high performance liquid chromatography (UHPLC). The error bar shows ± SD values of three biological and three technical replicates. DW dry weight

organs of the plants. A recent study conducted by Saxena et al. (2023a, b) indicates that *CaANS* exhibits elevated expression levels across various tissues, particularly within flower tissues. Conversely, *CaLAP2* demonstrated low expression levels during the flowering stages, with limited expression observed in the early stages of seed development. An earlier study by Nesi et al. (2001) shows that the TT2 expression was confined to the seed, overlapping with *BAN (BANYULS)* expression and PA deposition patterns. In the presence of a functional TT8 protein in *Arabidopsis*, the

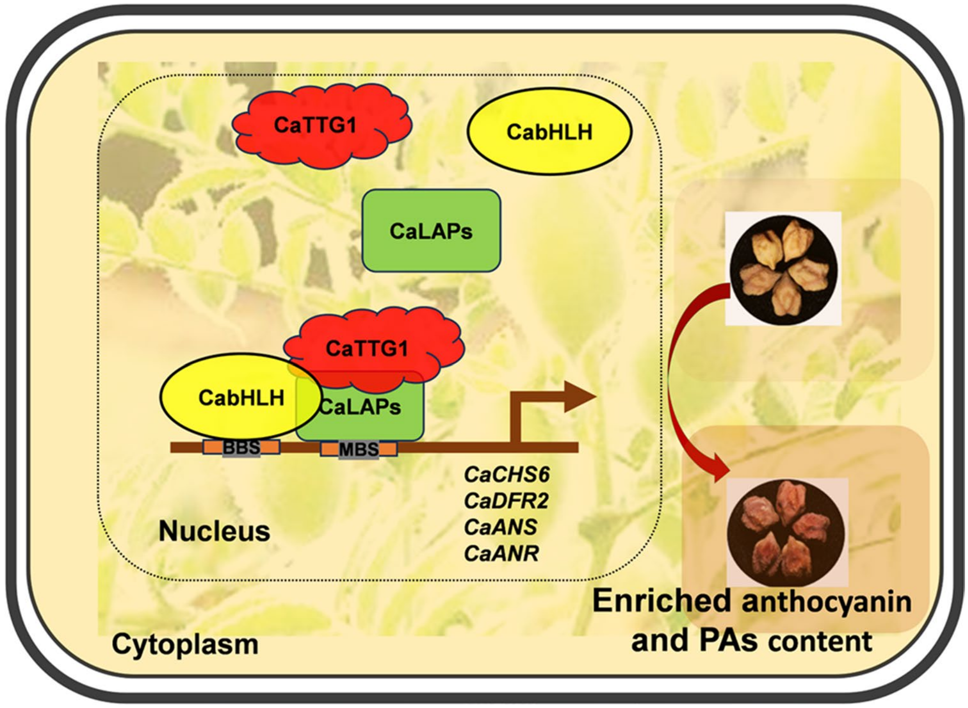

Fig. 8 Working model for the genetic manipulation of anthocyanin and PA biosynthesis in chickpea. CaLAP1/2 regulates the transcription of anthocyanin and PA biosynthetic genes leading to high anthocyanin and PA accumulation in the overexpression lines of chickpea. High anthocyanin accumulation in the *CaLAP1/2*-OE lines causes darker seed coat color. MBS, MYB-binding sites; *BBS* bHLH-binding sites; *CHS* chalcone synthase; *DFR* dihydroflavonol reductase; *ANS* anthocyanidin synthase; *ANR* anthocyanidin reductase

gain-of-function mutant TT2 could induce ectopic expression of *BAN* in young seedlings and roots in *Arabidopsis.*

R2R3-MYB and bHLH TFs play crucial roles in anthocyanin and PA accumulation. The MYB–bHLH complex is responsible for changes in the color phenotypes in different tissues of plants (An et al. 2020; Sun et al. 2021). Anthocyanin content modulated through transcriptional regulatory proteins inspired us to characterize the anthocyanin-specific R2R3-MYBs proteins in chickpea. In our study, we found that both CaLAP1 and CaLAP2 interact with CabHLH1 and CaTTG1 TFs to form a trimeric complex in chickpea. This finding aligns with previous research, which has shown that members of the SG6-R2R3-MYB, bHLH, and WD40 repeats protein families regulate anthocyanin biosynthesis across various plant species (Lin-Wang et al. 2010; Xie et al. 2020). Our investigation in chickpea, a key pulse crop with significant global utilization, highlights its crucial role in the study of anthocyanin regulation and biosynthesis. In *A. thaliana*, PAP1 (MYB) and EGL3 (bHLH) interact to form the MBW complex with TTG1 to regulate the biosynthesis of anthocyanins, while *TRANSPARENT TESTA2* (MYB) interacts with TT8 (bHLH) and TTG1 to regulate the biosynthesis of PA (Gonzalez et al. 2008; Li et al. 2020a, b). R2R3-MYB TFs harbor the conserved motif [D/E] LX2[R/K]X3LX6LX3R in the R3 domain, for the interaction with bHLH in addition to WD40 and form MBW complex that mediates anthocyanin biosynthesis (Kim et al. 2021). A similar kind of MBW regulatory module is known in different horticultural and flowering plant species where the SG6-R2R3-MYB TFs include Rosea1, Rosea2, and Venosa in *Antirrhinum majus,* MdMYB10 in apple, MYB75, MYB90, MYB113, and MYB114 in *Arabidopsis,* SlAN2-like in tomato, and VcMYBL1 in blueberry (Espley et al. 2007; Shang et al. 2011; Yan et. al 2020; Tang et al. 2021). Previous reports show that in *Oenanthe javanica,* OjMYB1 interacts with OjbHLH, and SmMYB75 interacts with TT8-like bHLH in eggplant which is responsible for regulating anthocyanin biosynthesis (Feng et al. 2018; Shi et al. 2021).

Co-transfection and dual-luciferase assays indicate that both CaLAP1 and CaLAP2 are independently capable of positively transactivating the activity of *CaCHS6, CaDFR2, CaANS,* and *CaANR* promoters. During co-infiltration with CabHLH1 and CaTTG1 proteins, the activity of the tested promoters significantly peaks, indicating the formation of a functional MBW complex. This suggests a synergistic interaction among these proteins in regulating gene expression. The heterologous expression of *CaLAP1* and *CaLAP2* in *A. thaliana myb* sextuple mutant suggests the partial restoration of anthocyanin in *Arabidopsis* seedlings. It might be due to the heterologous MBW complex formation from legume MYB and *Arabidopsis* EGL3 and TTG1 or due to the lower activity of MBW complex formed with a heterologous MYB protein on the promoters of *Arabidopsis* anthocyanin biosynthesis genes.

The transcript levels of anthocyanin-associated biosynthesis genes *CaDFR2* and *CaANS* which were exclusively higher during the flower and seed development stages showed a strong correlation with *CaLAP1* and *CaLAP2* expression, suggesting the regulatory role of CaLAP1 and

CaLAP2 in the reproductive organs. This data indicates increased levels of anthocyanins and PAs in seed coats, potentially contributing to protection against biotic stress (Ambawat et al. 2013). Indeed, the expression of *CaLAP1* and *CaLAP2* in flower and seed stages is higher and variable, which could be controlled by upstream activators or repressors transcriptionally and post-transcriptionally (Rajput et al. 2022a). Studies indicate that the accumulation of anthocyanins in chickpea plants is greatly influenced by the endogenous phytohormone content of the plant species (Brunetti et al. 2018 ; La Fountain et al. 2021). An et al. (2021) reported that the JAZ1 (JA-ZIM-domain)–TRB1(telomere-binding protein)–MYB9 module dynamically regulates the accumulation of anthocyanin and PA in response to jasmonic acid (JA) signaling. Auxin regulates the accumulation of anthocyanin and PA through the auxin response factor (ARF2), serving as a positive regulator of PAs, in *A. thaliana* (Jiang et al. 2022). The application of exogenous ethylene enhances anthocyanin accumulation in grape berries by promoting the transcription of key genes including *CHS, flavanone-3-hydroxylase* (*F3H*)*, leucocyanidin oxygenase* (*LDOX*)*, and UDP-glucose:flavonoid-3-O-glycosyltransferase* (*UFGT*) (El‐Kereamy et al. 2003).

Anthocyanins are essential for promoting plant reproduction, as their bright colors attract pollinators and seed dispersers (Petroni et al. 2011). Additionally, anthocyanins recurrently accumulate in young vegetative tissues and the sun-exposed tissues of fruits to guard against photoinhibition and photobleaching under light stress without significantly hampering photosynthesis (Gould et al. 2004). Light is a main environmental factor that affects anthocyanin levels, and HY5 controls the biosynthesis of anthocyanins by modulating the transcriptional activity of the MYB75/PAP1 TF in *Arabidopsis*, and B-box TF, MdBBX20 in apple, PpBBX18 and PpBBX21, associated with HY5 TFs in *Pyrus pyriflora* pear (Shin et al. 2013; Bai et al. 2019). Tomato *hy5 mutants* were generated using the CRISPR/Cas9 system to distinguish between HY5-dependent and -independent candidate TFs involved in anthocyanin biosynthesis (Qiu et al. 2019). In another study of the WRKY TF family, PyWRKY26 binds to the *PyMYB114* promoter in red-skinned pears and increases its expression, acting as an anthocyanin regulator (Li et al. 2020a, b). Additionally, MdHY5–MdWRKY41–MdMYB regulatory module affects apple fruits' anthocyanin and PA synthesis (Mao et al. 2021). Moreover, miR828 and miR858 are studied to target the coding sequence of anthocyanin-specific MYB repressors in grapes (Tirumalai et al. 2019).

Seeds from *CaLAP1* and *CaLAP2* overexpressing lines exhibit a darker hue compared to control seeds, yet maintain their seed weight and size. A comparable study in *Arabidopsis* reported that the lighter seed color resulting from AP2 (APETALA2) overexpression indicates a reduction in PA content, highlighting AP2 involvement in repressing PA biosynthesis. AP2 binds directly to the promoter of *MYBL2,* thereby enhancing its expression. Furthermore, AP2's interaction with MYBL2 inhibits the formation of the MBW complex (Jiang et al. 2023), further underscoring its regulatory influence on PA biosynthesis and anthocyanin-related pathways. Other TFs like TTG2 (WRKY) rely on the MBW trimeric complex and contribute to the accumulation of PAs in the *Arabidopsis* seed coat. Although the anthocyanin content and transcript of *CaDFR2* and *CaANS* are not well correlated in our results, it might be due to some post-transcriptional and post-translational changes occurring that might be modulating the anthocyanin content in the *CaLAP1* and *CaLAP2* overexpressing lines of chickpea. Jiang et al. (2020) reported that the MdMYB1 locus undergoes methylation because of apple Argonaute4 (MdAGO4s) binding to its promoter, thereby governing anthocyanin biosynthesis via the RNA-directed DNA methylation (RdDM) pathway.

The expression levels of anthocyanin and PA biosynthetic genes such as *CaANS, CaDFR2, CaANR,* and *CaLAR* are notably higher in the *CaLAP1* and *CaLAP2* overexpressing seed coats. Interestingly, some lines also exhibit higher expression in the embryo/cotyledon tissues. We observed that transgenic seeds exhibit a darker coloration compared to the wild type. Furthermore, the total anthocyanin and total PA content in these transgenic seeds are significantly higher, without adversely affecting seed size and weight. A similar kind of study reported in maize the function of *PALE ALEURONE COLOR1* (*PAC1*) is essential, as it codes for a WD40 repeat protein closely resembling AN11 and TTG1. *PAC1*'s involvement is vital for facilitating anthocyanin biosynthesis, particularly in the aleurone and scutellum of maize seeds. In our data. the variation in expression patterns suggests that seed coats may serve as storage tissues for anthocyanin and PA metabolites, serving as a buffer against various stresses and environmental challenges. Different forms of anthocyanins, including cyanidin, delphinidin, and petunidin, correlate well with the expression patterns of anthocyanin biosynthetic genes. Moreover, variations in anthocyanin content are observed within biological lines of *CaLAP1* and *CaLAP2* overexpression. Among the monomeric forms of PAs, such as catechin, epicatechin gallate, and epigallocatechin, higher accumulation is detected in transgenic lines, with catechin being a notably predominant PA, while the other two polymeric forms are of low level. This abundance of catechin provides robustness and protection against stress. Similar trends are observed in the accumulation of oligomeric forms of PAs in *CaLAP1* and *CaLAP2* overexpressing lines. This improvement in anthocyanin content, combined with elevated levels of PA, offers consumers access to seeds enriched with these beneficial compounds.

Moreover, higher levels of anthocyanins and proanthocyanins in transgenic seeds confer enhanced resistance to biotic and abiotic stresses. This attribute not only provides resistance in plants against various pathogens and environmental challenges, but also contributes to the overall health and resilience of the crop. The working model of the regulation of anthocyanin and PA in chickpea seed coats is also presented (Fig. 8). This model provides a comprehensive framework for genetically manipulating the anthocyanin production in chickpea to produce more nutritious crops enriched in anthocyanins and PAs. This can pave the way for future investigations into the role of R2R3-MYB TFs in different aspects of chickpea biology and crop improvement.

Supplementary Information The online version contains supplementary material available at https://doi.org/10.1007/s00425-024-04470-7.

Acknowledgements This work was supported by the core grant of National Institute of Plant Genome Research and Core Research Grant (CRG) from SERB-Department of Science and Technology (CRG/2022/001178) to AP. SS, LP, HC, and RR acknowledge UGC and the Council of Scientific and Industrial Research Government of India for Senior Research Fellowships. DC acknowledges the Department of Science and Technology, New Delhi, for financial support in the form of JC Bose National Fellowship (JCB/2020/000014). The authors are thankful to DBT-eLibrary Consortium (DeLCON) for providing access to e-resources.

Author contributions AP conceived the idea and designed the research. SS, LP, RR, HC, and NS performed the experiments. SS and AP wrote the manuscript. DC and AP edited and finalized the draft. All the authors have read and approved the manuscript for submission.

Data availability All data supporting the findings of this study are available within the manuscript and with the supplementary data provided.

Declarations

Conflict of interest The authors declare no conflict of interest.

References

Ambawat S, Sharma P, Yadav NR, Yadav RC (2013) MYB transcription factor genes as regulators for plant responses an overview. Physiol Mol Biol Plants 19:307–321

An JP, Xu RR, Liu X, Zhang JC, Wang XF, You CX, Hao YJ (2021) Jasmonate induces biosynthesis of anthocyanin and proanthocyanidin in apple by mediating the JAZ1–TRB1–MYB9 complex. Plant J 106:1414–1430

Appelhagen I, Jahns O, Bartelniewoehner L, Sagasser M, Weisshaar B, Stracke R (2011) Leucoanthocyanidin dioxygenase in *Arabidopsis thaliana*: characterization of mutant alleles and regulation by MYB–BHLH–TTG1 transcription factor complexes. Gene 484:61–68

Bac-Molenaar JA, Fradin EF, Rienstra JA, Vreugdenhil D, Keurentjes JJ (2015) GWA mapping of anthocyanin accumulation reveals balancing selection of MYB90 in *Arabidopsis thaliana*. PLoS ONE 10:e0143212

Bai S, Tao R, Yin L, Ni J, Yang Q, Yan X, Yang F, Guo X, Li H, Teng Y (2019) Two B-box proteins, PpBBX18 and PpBBX21, antagonistically regulate anthocyanin biosynthesis via competitive association with *Pyrus pyrifolia ELONGATED HYPOCOTYL 5* in the peel of pear fruit. Plant J 100:1208–1223

Bajaj D, Das S, Upadhyaya HD, Ranjan R, Badoni S, Kumar V, Parida SK (2015) A genome-wide combinatorial strategy dissects complex genetic architecture of seed coat color in chickpea. Front Plant Sci 6:979

Baudry A, Heim MA, Dubreucq B et al (2004) TT2, TT8, and TTG1 synergistically specify the expression of *BANYULS* and proanthocyanidin biosynthesis in *Arabidopsis thaliana*. Plant J 39:366–380

Bogs J, Downey MO, Harvey JS, Ashton AR, Tanner GJ, Robinson SP (2005) Proanthocyanidin synthesis and expression of genes encoding leucoanthocyanidin reductase and anthocyanidin reductase in developing grape berries and grapevine leaves. Plant Physiol 139:652–663

Borevitz JO, Xia Y, Blount J, Dixon RA, Lamb C (2000) Activation tagging identifies a conserved MYB regulator of phenylpropanoid biosynthesis. Plant Cell 12:2383–2393

Brunetti C, Fini A, Sebastiani F, Gori A, Tattini M (2018) Modulation of phytohormone signaling A primary function of flavonoids in plant–environment interactions. Front Plant Sci 9:1042

Carey CC, Strahle JT, Selinger DA, Chandler VL (2004) Mutations in the pale aleurone color1 regulatory gene of the *Zea mays* anthocyanin pathway have distinct phenotypes relative to the functionally similar *TRANSPARENT TESTA GLABRA1* gene in *Arabidopsis thaliana*. Plant Cell 16:450–464

Chen H, Zou Y, Shang Y, Lin H, Wang Y, Cai R, Tang X, Zhou JM (2008) Firefly luciferase complementation imaging assay for protein-protein interactions in plants. Plant Physiol 146:368–376

Chen CC, Lin C, Chen MH, Chiang PY (2019) Stability and quality of anthocyanin in purple sweet potato extracts. Foods 8:393

Clough SJ, Bent AF (1998) Floral dip a simplified method for *Agrobacterium*-mediated transformation of *Arabidopsis thaliana*. Plant J 16:735

Dasiman R, Nor NM, Esha Z, Mutalip SSM, Suwandi NR, Bidin H (2022) A review of procyanidin: Updates on current bioactivities and potential health benefits. Biointerface Res Appl Chem 12:5918–5940

Davies KM, Albert NW, Schwinn KE (2012) From landing lights to mimicry the molecular regulation of flower coloration and mechanisms for pigmentation patterning. Funct Plant Biol 39:61

Dixon RA, Paiva NL (1995) Stress-induced phenylpropanoid metabolism. Plant Cell 7:1085–1097

Dixon RA, Sarnala S (2020) Pdroanthocyanidin biosynthesis—a matter of protection. Plant Physiol 184:579–591

Dobin A, Davis CA, Schlesinger F et al (2013) STAR ultrafast universal RNA-seq aligner. Bioinformatics 29:15–21

Dubos C, Stracke R, Grotewold E et al (2010) MYB transcription factors in Arabidopsis. Trends Plant Sci 15:573–581. https://doi.org/10.1016/j.tplants.2010.06.005

Espley RV, Hellens RP, Putterill J, Stevenson DE, Kutty-Amma S, Allan AC (2007) Red colouration in apple fruit is due to the activity of the MYB transcription factor, MdMYB10. Plant J 49:414–427

Ezquerro M, Li C, Pérez-Pérez J, Burbano-Erazo E, Barja MV, Wang Y, Rodríguez-Concepción M (2023) Tomato geranylgeranyl diphosphate synthase isoform 1 is involved in the stress-triggered production of diterpenes in leaves and strigolactones in roots. New Phytol 239:2292–2306

Fang X, Shangguan L, Wang L (2023) MdMYB110a, directly and indirectly, activates the structural genes for the ALA-induced accumulation of anthocyanin in apple. Plant Sci 326:111511

Feng K, Xu ZS, Que F, Liu JX, Wang F, Xiong AS (2018) An R2R3-MYB transcription factor, OjMYB1, functions in anthocyanin biosynthesis in *Oenanthe javanica*. Planta 247:301–315

Garg R, Patel RK, Tyagi AK, Jain M (2011) De novo assembly of chickpea transcriptome using short reads for gene discovery and marker identification. DNA Res 18:53–63

Gonzalez A, Zhao M, Leavitt JM, Lloyd AM (2008) Regulation of the anthocyanin biosynthetic pathway by the TTG1/bHLH/Myb transcriptional complex in Arabidopsis seedlings. Plant J 53:814–827

Gould KS (2004) Nature's Swiss army knife the diverse protective roles of anthocyanins in leaves. J Biomed Biotechnol 5:314

Grasso N, Lynch NL, Arendt EK, Mahony O, JA, (2022) Chickpea protein ingredients A review of composition, functionality, and applications. Compr Rev Food Sci Food Saf 21:435–452

Haak M, Vinke S, Keller W et al (2018) High quality de novo transcriptome assembly of *Croton tiglium*. Front Mol Biosci 5:62

Hectors K, van Oevelen S, Guisez Y, Prinsen E, Jansen MA (2012) The phytohormone auxin is a component of the regulatory system that controls UV-mediated accumulation of flavonoids and UV-induced morphogenesis. Physiol Plant 145:594–603

Hu D-G, Sun C-H, Ma Q-J, You C-X, Cheng L, Hao YJ (2016) MdMYB1 regulates anthocyanin and malate accumulation by directly facilitating their transport into vacuoles in apples. Plant Physiol 170:1315–1330

Huang J, Gu M, Lai Z, Fan B, Shi K, Zhou YH, Chen Z (2010) Functional analysis of the Arabidopsis *PAL* gene family in plant growth, development, and response to environmental stress. Plant Physiol 153:1526–1538

Jameel S, Hameed A, Shah TM (2021) Biochemical profiling for antioxidant and therapeutic potential of Pakistani chickpea (*Cicer arietinum* L.) genetic resource. Front Plant Sci 12:663623

Jiang S, Wang N, Chen M, Zhang R, Sun Q, Xu H, Chen X (2020) Methylation of *MdMYB1* locus mediated by RdDM pathway regulates anthocyanin biosynthesis in apple. Plant Biotechnol J 18:1736–1748

Jiang W, Xia Y, Su X, Pang Y (2022) ARF2 positively regulates flavonols and proanthocyanidins biosynthesis in *Arabidopsis thaliana*. Planta 256:44

Jiang W, Yin Q, Liu J, Su X, Han X, Li Q, Pang Y (2023) The APETALA2–MYBL2 module represses proanthocyanidin biosynthesis by affecting formation of the MBW complex in seeds of *Arabidopsis thaliana*. Plant Commun 5(3):100777

Jideani AI, Silungwe H, Takalani T, Omolola AO, Udeh HO, Anyasi TA (2021) Antioxidant-rich natural fruit and vegetable products and human health. Int J Food Prop 24:41–67

Katoh K, Standley DM (2013) MAFFT multiple sequence alignment software version 7 improvements in performance and usability. Mol Biol Evol 30:772–780

Khandal H, Gupta SK, Dwivedi V et al (2020) Root-specific expression of chickpea cytokinin oxidase/ dehydrogenase 6 leads to enhanced root growth, drought tolerance and yield without compromising nodulation. Plant Biotechnol J 18:2225–2240

Kim DH, Lee J, Rhee J, Lee JY, Lim SH (2021) Loss of the R2R3 MYB transcription factor RsMYB1 shapes anthocyanin biosynthesis and accumulation in *Raphanus sativus*. Int J Mol Sci 22:10927

Koncz C, Schell J (1986) The promoter of TL-DNA gene 5 controls the tissue-specifc expression of chimeric genes carried by a novel type of *Agrobacterium* binary vector. Mol Gen Genet 204:383–396

Koul B, Sharma K, Sehgal V, Yadav D, Mishra M, Bharadwaj C (2022) Chickpea (*Cicer arietinum* L.) biology and biotechnology from domestication to biofortification and biopharming. Plants 11:2926

Kumar K, Purayannur S, Kaladhar VC et al (2018) mQTL-seq and classical mapping implicates the role of an *AT-HOOK MOTIF CONTAINING NUCLEAR LOCALIZED* (*AHL*) family gene in Ascochyta blight resistance of chickpea. Plant Cell Environ 41:2128–2140

LaFountain AM, Yuan YW (2021) Repressors of anthocyanin biosynthesis. New Phytol 231:933–949

Lattanzio V, Kroon PA, Quideau S, Treutter D (2009) Plant phenolics—secondary metabolites with diverse functions. Recent Adv Polyphen Res 1:1–35

Li L, Ban ZJ, Li XH, Wu MY, Wang AL, Jiang YQ, Jiang YH (2012) Differential expression of anthocyanin biosynthetic genes and transcription factor PcMYB10 in pears (*Pyrus communis* L.). PLoS ONE 7:e46070

Li P, Chen B, Zhang G, Chen L, Dong Q, Wen J, Zhao J (2016) Regulation of anthocyanin and proanthocyanidin biosynthesis by *Medicago truncatula* bHLH transcription factor MtTT8. New Phytol 210:905–921

Li SF, Allen PJ, Napoli RS, Browne RG, Pham H, Parish RW (2020a) MYB–bHLH–TTG1 regulates a Arabidopsis seed coat biosynthesis pathways directly and indirectly via multiple tiers of transcription factors. Plant Cell Physiol 61:1005–1018

Li C, Wu J, Hu KD, Wei SW, Sun HY, Hu LY, Han Z, Yao GF, Zhang H (2020b) *PyWRKY26* and *PybHLH3* cotargeted the *PyMYB114* promoter to regulate anthocyanin biosynthesis and transport in red-skinned pears. Hortic Res 7:37

Liao Y, Smyth GK, Shi W (2014) feature Counts: an efficient general purpose program for assigning sequence reads to genomic features. Bioinformatics 30:923–930

Lin-Wang K, Bolitho K, Grafton K et al (2010) An R2R3 MYB transcription factor associated with regulation of the anthocyanin biosynthetic pathway in Rosaceae. BMC Plant Biol 10:50

Liu Y, Hou H, Jiang X, Wang P, Dai X, Chen W, Xia T (2018) A WD40 repeat protein from *Camellia sinensis* regulates anthocyanin and proanthocyanidin accumulation through the formation of MYB–bHLH–WD40 ternary complexes. Int J Mol Sci 19:1686

Livak KJ, Schmittgen TD (2001) Analysis of relative gene expression data using real-time quantitative PCR and the 2−ΔΔCT method. Methods 25:402–408

Mao Z, Jiang H, Wang S, Wang Y, Yu L, Zou Q, Liu W, Jiang S, Wang N, Zhang Z, Chen X (2021) The MdHY5–MdWRKY41–MdMYB transcription factor cascade regulates the anthocyanin and proanthocyanidin biosynthesis in red-fleshed apple. Plant Sci 306:110848

Martin K, Kopperud K, Chakrabarty R et al (2009) Transient expression in *Nicotiana benthamiana* fuorescent marker lines provides enhanced definition of protein localization, movement and interactions in planta. Plant J 59:150–162

Mellway RD, Tran LT, Prouse MB, Campbell MM, Constabel CP (2009) The wound-, pathogen-, and ultraviolet B-responsive *MYB134* gene encodes an R2R3 MYB transcription factor that regulates proanthocyanidin synthesis in poplar. Plant Physiol 150:924–941

Misra P, Pandey A, Tiwari M, Chandrashekar K, Sidhu OP, Asif MH, Tuli R (2010) Modulation of transcriptome and metabolome of tobacco by Arabidopsis transcription factor, *AtMYB12*, leads to insect resistance. Plant Physiol 152:2258–2268

Muñoz-Gómez S, Suárez-Baron H, Alzate JF, González F, Pabón-Mora N (2021) Evolution of the subgroup 6 *R2R3-MYB* genes and their contribution to floral color in the Perianth-bearing Piperales. Front Plant Sci 12:633227

Naik J, Rajput R, Pucker B, Stracke R, Pandey A (2021) The R2R3-MYB transcription factor MtMYB134 orchestrates flavonol biosynthesis in *Medicago truncatula*. Plant Mol Biol 106:157–172

Naik J, Misra P, Trivedi PK, Pandey A (2022) Molecular components associated with the regulation of flavonoid biosynthesis. Plant Sci 317:111196

Naik J, Tyagi S, Rajput R, Kumar P, Pucker B, Bisht NC, Pandey A (2024) Flavonols affect the interrelated glucosinolate and camalexin biosynthetic pathways in *Arabidopsis thaliana*. J Exp Bot 75(1):219–240

Nakagawa T, Kurose T, Hino T et al (2007) Development of series of gateway binary vectors, pGWBs, for realizing efficient construction of fusion genes for plant transformation. J Biosci Bioeng 104:34–41

Nesi N, Jond C, Debeaujon I, Caboche M, Lepiniec L (2001) The Arabidopsis *TT2* gene encodes an R2R3 MYB domain protein that acts as a key determinant for proanthocyanidin accumulation in developing seed. Plant Cell 13:2099–2114

Pal L, Dwivedi V, Gupta SK, Saxena S, Pandey A, Chattopadhyay D (2023) Biochemical analysis of anthocyanin and proanthocyanidin and their regulation in determining chickpea flower and seed coat colour. J Exp Bot 74:130–148

Pandey A, Misra P, Bhambhani S, Bhatia C, Trivedi PK (2014) Expression of *Arabidopsis* MYB transcription factor, *AtMYB111*, in tobacco requires light to modulate flavonol content. Sci Rep 4:5018

Pandey A, Misra P, Trivedi PK (2015) Constitutive expression of *Arabidopsis* MYB transcription factor, *AtMYB11*, in tobacco modulates flavonoid biosynthesis in favor of flavonol accumulation. Plant Cell Rep 34:1515–1528

Pandey A, Alok A, Lakhwani D, Singh J, Asif MH, Trivedi PK (2016) Genome-wide expression analysis and metabolite profiling elucidate transcriptional regulation of flavonoid biosynthesis and modulation under abiotic stresses in banana. Sci Rep 6:31361

Pang Y, Peel GJ, Wright E et al (2007) Early steps in proanthocyanidin biosynthesis in the model legume *Medicago truncatula*. Plant Physiol 145:601–615

Paolocci F, Robbins MP, Passeri V, Hauck B, Morris P, Rubini A, Arcioni S, Damiani F (2011) The strawberry transcription factor FaMYB1 inhibits the biosynthesis of proanthocyanidins in *Lotus corniculatus* leaves. J Exp Bot 62:1189–1200

Peel GJ, Pang Y, Modolo LV, Dixon RA (2009) The LAP1 MYB transcription factor orchestrates anthocyanidin biosynthesis and glycosylation in *Medicago*. Plant J 59:136–149

Pérez-Díaz JR, Pérez-Díaz J, Madrid-Espinoza J, González-Villanueva E, Moreno Y, Ruiz-Lara S (2016) New member of the R2R3-MYB transcription factors family in grapevine suppresses the anthocyanin accumulation in the flowers of transgenic tobacco. Plant Mol Biol 90:63–76

Petroni K, Tonelli C (2011) Recent advances on the regulation of anthocyanin synthesis in reproductive organs. Plant Sci 181:219–229

Pipas JM, Levine AJ (2001) Role of T antigen interactions with p53 in tumorigenesis. Semin Cancer Biol 11:23–30

Qi Q, Chu M, Yu X, Xie Y, Li Y, Du Y, Yan N (2023) Anthocyanins and proanthocyanidins: chemical structures, food sources, bioactivities, and product development. Food Rev Int 39:4581–4609

Qiu Z, Wang H, Li D, Bingwei Y, Hui Q, Yan S, Huang Z, Cui X, Cao B (2019) Identification of candidate HY5-dependent and independent regulators of anthocyanin biosynthesis in tomato. Plant Cell Physiol 60:643–656

Rajkumar MS, Gupta K, Khemka NK, Garg R, Jain M (2020) DNA methylation reprogramming during seed development and its functional relevance in seed size/weight determination in chickpea. Commun Biol 3:1–3

Rajput R, Naik J, Pandey SR, A, (2022a) Interplay between R2R3 MYB-type activators and repressors regulates proanthocyanidin biosynthesis in banana (*Musa acuminata*). New Phytol 236:1108–1127

Rajput R, Tyagi S, Naik J, Pucker B, Stracke R, Pandey A (2022b) The R2R3-MYB gene family in *Cicer arietinum* genome-wide identification and expression analysis leads to functional characterization of proanthocyanidin biosynthesis regulators in the seed coat. Planta 256:67

Ramsay NA, Glover BJ (2005) MYB–bHLH–WD40 protein complex and the evolution of cellular diversity. Trends Plant Sci 10:63–70

Redondo-Gómez S (2013) Abiotic and biotic stress tolerance in plants. In: Rout G, Das A (eds) Molecular stress physiology of plants. Springer, India, Pp, pp 1–20. https://doi.org/10.1007/978-81-322-0807-5_1

Rinaldo AR, Cavallini E, Jia Y, Moss SM, McDavid DA, Hooper LC, Robinson SP, Tornielli GB, Zenoni S, Ford CM, Boss PK (2015) A grapevine anthocyanin acyltransferase, transcriptionally regulated by VvMYBA, can produce most acylated anthocyanins present in grape skins. Plant Physiol 169:1897–1916

Samanta A, Das G, Das SK (2011) Roles of flavonoids in plants. Carbon 100:12–35

Saxena S, Pal L, Naik J, Singh Y, Verma PK, Chattopadhyay D, Pandey A (2023a) The R2R3-MYB-SG7 transcription factor CaMYB39 orchestrates surface phenylpropanoid metabolism and pathogen resistance in chickpea. New Phytol 238:798–816

Saxena S, Pal G, Pandey A (2023b) Functional characterization of 2-oxoglutarate-dependent dioxygenase gene family in chickpea. Plant Sci 336:111836

Seo J, Gordish-Dressman H, Hofman EP (2006) An interactive power analysis tool for microarray hypothesis testing and generation. Bioinformatics 22:808–814

Shang Y, Venail J, Mackay S, Bailey PC, Schwinn KE, Jameson PE, Martin CR, Davies KM (2011) The molecular basis for venation patterning of pigmentation and its effect on pollinator attraction in flowers of *Antirrhinum*. New Phytol 189:602–615

Shi S, Liu Y, He Y, Li L, Li D, Chen H (2021) R2R3-MYB transcription factor SmMYB75 promotes anthocyanin biosynthesis in eggplant (*Solanum melongena* L.). Scientia Hortic 282:110020

Shin DH, Choi M, Kim K, Bang G, Cho M, Choi SB, Choi G, Park YI (2013) HY5 regulates anthocyanin biosynthesis by inducing the transcriptional activation of the MYB75/PAP1 transcription factor in *Arabidopsis*. FEBS Lett 587:1543–1547

Stracke R, Ishihara H, Huep G, Barsch A, Mehrtens F, Niehaus K, Weisshaar B (2007) Differential regulation of closely related R2R3-MYB transcription factors controls flavonol accumulation in different parts of the *Arabidopsis thaliana* seedling. Plant J 50:660–677

Stracke R, Jahns O, Keck M et al (2010) Analysis of production of flavonol glycosides-dependent flavonol glycoside accumulation in *Arabidopsis thaliana* plants reveals MYB11, MYB12, and MYB111-independent flavonol glycoside accumulation. New Phytol 188:985–1000

Stracke R, Thiedig K, Kuhlmann M, Weisshaar B (2016) Analyzing synthetic promoters using Arabidopsis protoplasts. In: Hehl R (eds) Plant synthetic promoters. Methods in molecular biology, vol 1482. Humana Press, New York, NY, pp 67–81

Tang Q, Chi FM, Liu HD, Zhang HJ, Song Y (2021) Single-molecule real-time and Illumina sequencing to analyze transcriptional regulation of flavonoid synthesis in blueberry. Front Plant Sci 12:754325

Tirumalai V, Swetha C, Nair A, Pandit A, Shivaprasad PV (2019) miR828 and miR858 regulate VvMYB114 to promote anthocyanin and flavonol accumulation in grapes. J Exp Bot 70:4775–4792

Tohge T, de Souza LP, Fernie AR (2017) Current understanding of the pathways of flavonoid biosynthesis in model and crop plants. J Exp Bot 68:4013–4028

Wang Y, Yin H, Long Z, Zhu W, Yin J, Song X, Li C (2022) DhMYB2 and DhbHLH1 regulates anthocyanin accumulation via activation of late biosynthesis genes in *Phalaenopsis*-type *Dendrobium*. Front Plant Sci 13:1046134

Xie S, Lei Y, Chen H, Li J, Chen H, Zhang Z (2020) R2R3-MYB transcription factors regulate anthocyanin biosynthesis in grapevine vegetative tissues. Front Plant Sci 11:527

Yan S, Chen N, Huang Z, Li D, Zhi J, Yu B, Liu X, Cao B, Qiu Z (2020) *Anthocyanin Fruit* encodes an R2R3-MYB transcription factor, SlAN2-like, activating the transcription of *SlMYBATV* to fine-tune anthocyanin content in tomato fruit. New Phytol 225:2048–2063

Yue M, Jiang L, Zhang N, Zhang L, Liu Y, Lin Y, Tang H (2023) Regulation of flavonoids in strawberry fruits by FaMYB5/FaMYB10 dominated MYB–bHLH–WD40 ternary complexes. Front Plant Sci 14:1145670

Zimmermann IM, Heim MA, Weisshaar B, Uhrig JF (2004) Comprehensive identification of *Arabidopsis thaliana* MYB transcription factors interacting with R/B-like BHLH proteins. Plant J 40:22–34

Zuluaga DL, Gonzali S, Loreti E, Pucciariello C, Degl'Innocenti E, Guidi L, Alpi A, Perata P (2008) *Arabidopsis thaliana* MYB75/PAP1 transcription factor induces anthocyanin production in transgenic tomato plants. Funct Plant Biol 35:606–618